



HAL
open science

The BRAHMA-associated SWI/SNF chromatin remodeling complex controls Arabidopsis seed quality and physiology

Magdalena Wrona, Julia Zinsmeister, Michal Krzyszton, Claire Villette, Julie Zumsteg, Pierre Mercier, Martine Neveu, Sebastian Sacharowski, Rafal Archacki, Boris Collet, et al.

► **To cite this version:**

Magdalena Wrona, Julia Zinsmeister, Michal Krzyszton, Claire Villette, Julie Zumsteg, et al.. The BRAHMA-associated SWI/SNF chromatin remodeling complex controls Arabidopsis seed quality and physiology. *Plant Physiology*, 2024, 10.1093/plphys/kiae642 . hal-04842520

HAL Id: hal-04842520

<https://hal.science/hal-04842520v1>

Submitted on 19 Dec 2024

HAL is a multi-disciplinary open access archive for the deposit and dissemination of scientific research documents, whether they are published or not. The documents may come from teaching and research institutions in France or abroad, or from public or private research centers.

L'archive ouverte pluridisciplinaire **HAL**, est destinée au dépôt et à la diffusion de documents scientifiques de niveau recherche, publiés ou non, émanant des établissements d'enseignement et de recherche français ou étrangers, des laboratoires publics ou privés.



Distributed under a Creative Commons Attribution 4.0 International License

1 **The BRAHMA-associated SWI/SNF chromatin remodeling complex controls Arabidopsis**
2 **seed quality and physiology**

3

4

5 Magdalena Wrona^{1,*}, Julia Zinsmeister^{1¶*}, Michal Krzyszton¹, Claire Villette², Julie Zumsteg²,
6 Pierre Mercier², Martine Neveu⁴, Sebastian P. Sacharowski¹, Rafał Archacki³, Boris Collet⁵, Julia
7 Buitink⁴, Hubert Schaller², Szymon Swiezewski^{1,#} and Ruslan Yatusevich^{1,#}

8

9 ¹ Institute of Biochemistry and Biophysics PAS, Warsaw 02-106, Poland

10

11 ² Institut de Biologie Moléculaire des Plantes, Université de Strasbourg, Strasbourg 67084,
12 France

13

14 ³ Laboratory of Systems Biology, Faculty of Biology, University of Warsaw, Warsaw 02-096,
15 Poland

16

17 ⁴ INRAE, Institut Agro, Université d'Angers, IRHS, Angers 49000, France

18

19 ⁵ Université Paris Saclay, INRAE, AgroParisTech, Institute Jean-Pierre Bourgin for Plant
20 Sciences (IJPB), 78000, Versailles, France.

21

22 [¶] Present address: INRAE Centre IdF de Versailles-Saclay, Versailles Cedex 78026, France

23 * These authors contributed equally

24

25

26 [#] Corresponding authors: sswicz@ibb.waw.pl (S.S), yatusev@gmail.com (R.Y.)

27

28 **Short title:** BRM controls seed biology through *asDOG1*

32

33 The authors responsible for distribution of materials integral to the findings presented in this
34 article in accordance with the policy described in the Instructions for Authors

1

35 (<https://academic.oup.com/plphys/pages/General-Instructions>) are Szymon Swiezewski and
36 Ruslan Yatusevich.

37

38 **Abstract**

39 The SWI/SNF (SWItch/Sucrose Non-Fermentable) chromatin remodeling complex is
40 involved in various aspects of plant development and stress responses. Here, we investigated
41 the role of BRM (BRAHMA), a core catalytic subunit of the SWI/SNF complex, in
42 *Arabidopsis thaliana* seed biology. *brm-3* seeds exhibited enlarged size, reduced yield,
43 increased longevity, and enhanced secondary dormancy, but did not show changes in primary
44 dormancy or salt tolerance. Some of these phenotypes depended on the expression of *DOG1*,
45 a key regulator of seed dormancy, as they were restored in the *brm-3 dog1-4* double mutant.
46 Transcriptomic and metabolomic analyses revealed that BRM and DOG1 synergistically
47 modulate the expression of numerous genes. Some of the changes observed in the *brm-3*
48 mutant, including increased glutathione levels, depended on a functional *DOG1*. We
49 demonstrated that the BRM-containing chromatin remodeling complex directly controls
50 secondary dormancy through *DOG1* by binding and remodeling its 3' region, where the
51 promoter of the long non-coding RNA *asDOG1* is located. Our results suggest that BRM and
52 DOG1 cooperate to control seed physiological properties and that BRM regulates *DOG1*
53 expression through *asDOG1*. This study reveals chromatin remodeling at the *DOG1* locus as
54 a molecular mechanism controlling the interplay between seed viability and dormancy.

55 Introduction

56 Seeds encapsulate plant embryos in a state of suspended development, poised to resume life cycle
57 upon encountering favorable environmental conditions. Many plant species, including
58 *Arabidopsis thaliana*, produce seeds that can be stored in a dry stage for an extended time. This
59 ability is known as seed longevity. In addition, seeds can also postpone germination despite
60 optimal conditions, in a process known as dormancy that helps to adjust germination capability to
61 changes in the environment. Dormancy established during seed maturation is known as primary
62 dormancy, and is defined as a state in which freshly harvested seeds cannot germinate even under
63 favorable conditions. Primary dormancy can be relieved by different means including after
64 ripening – dry storage, or stratification – exposure to cold in the imbibed state. In contrast,
65 dormancy developed by a non-dormant, imbibed seed in response to an unfavorable germination
66 condition is known as secondary dormancy (Cadman *et al.*, 2006; Finch-Savage & Leubner-
67 Metzger, 2006; Baskin & Baskin, 2014).

68 *DELAY OF GERMINATION1* gene (*DOG1*), the main regulator of seed dormancy, has been
69 identified by population analysis (Bentsink *et al.*, 2006) and further characterized in numerous
70 molecular studies (Carrillo-Barral *et al.*, 2020). Primary dormancy and longevity are both
71 acquired during seed development and are strictly regulated by numerous external and internal
72 factors (Holdsworth *et al.*, 2008; Sano *et al.*, 2016). Interestingly, in *Arabidopsis* a trade-off
73 between seed longevity and dormancy was described, as deep dormancy was associated with low
74 longevity, suggesting that longevity and dormancy are genetically negatively correlated. On the
75 contrary, *DOG1* has been shown to act as a positive regulator of both dormancy and longevity as
76 *dog1* mutants show low primary and secondary dormancy as well as low longevity (Nguyen *et al.*
77 *et al.*, 2012; Dekkers *et al.*, 2013; Footitt *et al.*, 2015). As a central regulator of seed biology, *DOG1*
78 expression is extensively regulated (Tognacca & Botto, 2021). Known regulators include two
79 long non-protein coding RNA (lncRNA): one is the *PUPPIES* that activates *DOG1* expression
80 and is transcribed from the *DOG1* promotor (Montez *et al.*, 2023) and a second is *asDOG1* that is
81 transcribed from within the *DOG1* intron 2 in antisense orientation and suppresses *DOG1*
82 expression (Fedak *et al.*, 2016).

83 Secondary dormancy modulation underlies the dormancy cycling phenomena described for seeds
84 forming soil seed banks (Footitt *et al.*, 2015, 2017). Analysis of histone posttranslational
85 modifications at the *DOG1* gene during dormancy cycling has led to a model where chromatin
86 remodeling at the *DOG1* locus underpins this process (Footitt *et al.*, 2015). Compared to primary

87 dormancy, the mechanisms of secondary dormancy establishment in various plant species
88 including *Arabidopsis thaliana* are mostly uncharted. Only few regulators have been identified so
89 far and most of them influence both primary and secondary dormancy (Skubacz & Daszkowska-
90 Golec, 2017; Buijs, 2020). Both types of dormancy are intricately modulated by environmental
91 cues, such as variations in light quality, moisture levels, and transient cold exposure. They are
92 also dependent on internal hormones, namely gibberellic acid (GA) and abscisic acid (ABA,
93 Hauvermale *et al.*, 2015; Sano & Marion-Poll, 2021). ABA plays a pivotal role in initiating and
94 sustaining dormancy, while GA acts as the trigger that breaks dormancy and promotes the
95 germination process (Iwasaki *et al.*, 2022).

96 SWI/SNF (SWIth/Sucrose Non-Fermentable) is a highly conserved chromatin-remodeling
97 complex that uses ATP to remodel chromatin. SWI/SNF complexes have been implicated in the
98 control of multiple developmental processes and in orchestrating responses to environmental
99 stimuli in yeast, plants, and animals (Ojolo *et al.*, 2018; Hernández-García *et al.*, 2022;
100 Bieluszewski *et al.*, 2023). In *Arabidopsis*, several homologous subunits of the SWI/SNF
101 complex have been described and many of these subunits are encoded by gene families, including
102 SNF2-type ATPases: SPLAYED (SYD), BRAHMA (BRM), CHR12/MINU1 and
103 CHR23/MINU2 (Shang & He, 2022; Guo *et al.*, 2022a). These subunits create the basis for plant
104 SWI/SNF complex taxonomy dividing them into BRM-associated (BAS), SYD-associated (SAS)
105 and MINU-associated (MAS) (Guo *et al.*, 2022b; Fu *et al.*, 2023). The BRM-containing complex
106 (BAS) is probably the best-studied chromatin remodeling complex in plants. BRM ATPase
107 contains multiple protein domains, including a bromodomain that binds acetylated histones and is
108 thought to facilitate the complex recruitment to targeted DNA. In addition to BRM, the BAS
109 complex contains other bromodomain-containing proteins - BRDs (BRD1/2/13) (Jarończyk *et al.*
110 *et al.*, 2021). Studies of *Arabidopsis* mutants of BAS complex subunits have shown that the BRM
111 containing BAS-SWI/SNF complex is involved in multiple environmental responses and
112 developmental transitions including seed maturation, embryogenesis, cotyledon separation, leaf
113 development, root stem cell maintenance, floral patterning or flowering (Yu *et al.*, 2021; Shang
114 & He, 2022; Guo *et al.*, 2022b; Bieluszewski *et al.*, 2023). Consistent with these findings,
115 *Arabidopsis brm* knockout mutants (*brm-1*) display severe phenotypes including dwarfism, leaf
116 curling, and sterility (Farrona *et al.*, 2004). Conversely, the *brm-3* mutant, which lacks the
117 bromodomain in the BRM protein, is not sterile and exhibits mild phenotypic abnormalities,
118 including seed coat defects (Hurtado *et al.*, 2006; Farrona *et al.*, 2007). Similar analysis of single
119 and multiple mutants of the *BRD1/2/13* genes revealed their redundant role in regulating

120 vegetative development, flowering, as well as the responses to GA and ABA hormones
121 (Jarończyk *et al.*, 2021; Stachula *et al.*, 2023). Despite the extensive work describing SWI/SNF
122 and BRM's role in seeds development and germination (Han *et al.*, 2012; Ding *et al.*, 2022), the
123 role of the BAS complex in seed biology remains poorly understood.

124 We and others showed before that apart from promoter regions, chromatin remodelers exhibit
125 extensive binding at the 3'ends of genes (Brzezinka *et al.*, 2016; Archacki *et al.*, 2016; Jégu *et al.*
126 *et al.*, 2017). This led us to hypothesize that the BAS-containing SWI/SNF complex may regulate
127 antisense transcription to indirectly control the sense gene expression (Archacki *et al.*, 2016). A
128 reporter-effector study in young Arabidopsis seedlings identified *DOG1* as one of the genes
129 displaying BRM binding at the 3'end (Archacki *et al.*, 2016). Here, we asked whether the link
130 between BRM and *DOG1* may be important in seeds where the role of *DOG1* and its regulation
131 through *asDOG1* is well established (Fedak *et al.*, 2016). Here we show that BRM is implicated
132 in multiple aspects of seed biology including seed size, seed longevity and seed dormancy. We
133 demonstrate that some of the affected seed properties, including dormancy, are *DOG1* dependent
134 and that the BAS complex controls secondary dormancy but not primary seed dormancy through
135 *asDOG1* antisense transcription.

136 **Results**

137 **BRM-mediated gene expression and metabolite composition in mature Arabidopsis seeds**

138 To investigate the role of BRM in Arabidopsis seed biology in the context of *DOG1*, we created
139 *brm-3dog1-4* double mutant and compared it with the wild type and single mutants in
140 downstream analyses. *BRM* knockout allele *brm-1* is sterile, we therefore used the T-DNA
141 insertion line *brm-3* (Tang *et al.*, 2008) and the double mutant *brm-3dog1-4*. 3'RNA-seq data
142 analysis identified 77, 211 and 911 transcripts with decreased transcript levels in *brm-3*, *dog1-4*
143 and *brm-3dog1-4*, respectively, and 167, 385 and 1391 transcripts with increased expression
144 (absolute fold change > 1, FDR < 0.05) (Fig. 1A). As expected, comparison of differentially
145 expressed genes in *brm-3* and *dog1-4* single mutants showed strong overlap with genes
146 misregulated in double *brm-3dog1-4* mutant (Fig. 1B, Supplementary Figure S1C). Moreover,
147 genes misregulated in *brm-3* and *dog1-4* also showed a substantial overlap (Fig. 1B).
148 Interestingly, *dog1-4*, *brm-3* and double *brm-3dog1-4* mutants showed a substantial number of
149 genes misregulated in the same directions (up and/or down), suggesting that *DOG1* and *BRM* act
150 synergistically in controlling gene expression in seeds (Fig. 1B). Self-clustering of expression
151 profiles among genes misregulated in *brm-3* identified nine groups of genes (Fig.1C). Three

152 groups showed opposite changes in *brm-3* and *dog1-4* and at least partial suppression of the *brm*
153 mutation-caused defects in the double *brm-3dog1-4* mutant (Fig.1C). Based on this, we
154 considered the BRM effect on those genes as *DOG1*-gene dependent (Fig. 1C, D).

155 Transcriptomic analysis showed that both BRM and DOG1 are important players in seed biology
156 and gene expression regulation. Our data revealed that in seeds, BRM and DOG1 control
157 expression of a large number of genes synergistically. There is, however, a substantial subset (55
158 out of 244) of genes that are regulated by BRM in DOG1 dependent manner (Fig. 1C, 1D).

159 Gene Ontology (GO) analysis identified 20 and 30 significantly enriched GO terms among genes
160 that were down- and up-regulated in the *brm-3* mutant, respectively. Among those, many GO
161 terms represented molecular functions involved in response to oxidative stress, with some related
162 to glutathione metabolism, binding and transferase activity, which are essential for the control of
163 reactive oxygen species (ROS) (Supplementary Table 1). Single *dog1-4* mutant and *brm-3dog1-4*
164 double mutant showed similar GO term profiles. Those included response to multiple factors, like
165 stimulus or ABA for down-regulated genes (Supplementary Fig. S2A), as well as GO terms
166 related to translation – for up-regulated genes (Supplementary Table 1).

167 Next, we analyzed the metabolic profiles of *brm-3*, *dog1-4* and *brm-3dog1-4* double mutant
168 mature seeds using a non-targeted comparative metabolomics approach based on high-resolution
169 mass spectrometry. Molecular features detected in each single mutant and in the double mutant
170 *brm-3dog1-4* were compared to Col-0 wild type (WT). This identified a total of 410, 112 and 418
171 differentially abundant molecular features (metabolites) in *brm-3*/WT, *dog1-4*/WT and *brm-3*
172 *3dog1-4*/WT comparisons, respectively (Wilcoxon rank sum test, fold change \geq 2; p-value $<$ 0.05,
173 Supplementary Fig. S1). Among them, 223 were more abundant and 187 were less abundant in
174 *brm-3* in comparison to Col-0 WT. In *dog1-4* mutant, 30 were more and 82 less abundant when
175 compared to WT. Finally, in the double mutant, 254 metabolites were more, and 164 were less
176 abundant when compared to Col-0 WT, indicating a significant metabolic remodeling in *brm-3*
177 and *brm-3dog1-4* mutants. Assigned masses allowed us to identify a putative molecular formula
178 for 170 out of 410 differentially expressed metabolites for *brm-3*/WT, 37 out of 112 for *dog1-*
179 *4*/WT and 143 out of 418 compounds for double mutant (Supplementary Table 1). To visualize
180 the metabolic changes between mutants and the Col-0 WT, we used a chemical enrichment
181 analysis named ChemRICH (Chemical Similarity Enrichment Analysis for Metabolites)
182 according to Barupal and Fiehn, 2017, which provides differentially enriched clusters of
183 metabolites families. Such clusters were identified for each mutant separately (Fig. 1E and

184 Supplementary Table 1). For *brm-3*, we detected 26 differentially abundant metabolic families
185 (p-value<0.05), with a decrease in compounds such as phosphatidylcholine,
186 phosphatidylethanolamine, aldehydes, flavonoids and glucosinolates and an enrichment of
187 indoles, polyunsaturated alkamides, phenols, unsaturated fatty acids and amides (Fig. 1E).
188 Interestingly, a 1.6 FC (p-value=0.0012) enrichment in glutathione was found in *brm-3* mutant
189 compared to Col-0 WT (Fig. 1F, Supplementary Table 1). Similarly, in the seeds of the *dog1-4*
190 mutant metabolomic analysis revealed decrease in flavonoids and peptides levels and an
191 enrichment in phenols and glucosides (Fig. 1E). Interestingly, in *dog1-4* mutant we found a -2.08
192 FC decrease (p-value=0.0059) in glutathione enrichment compared to Col-0 (Fig. 1E, 1F). In the
193 double mutant *brm-3dog1-4*, we found a broad variety of metabolic families up or downregulated
194 compared to Col-0 WT. We noticed an enrichment in phospholipids ethers, phenols, saturated
195 and unsaturated lysophosphatidylcholine, lactones, saturated fatty acids and indoles; and lower
196 levels of phosphatidylcholine, phosphatidylethanolamine, glucosinolates, flavonoids and
197 glucosides (Supplementary Table 1). Interestingly, as observed for the single mutants, the double
198 mutant glutathione was downregulated compared to the wild type (Fig. 1E, 1F, Supplementary
199 Table 1), with a FC of -1.85 (p-value=0.00058). We conclude that similarly to RNA-seq
200 analysis, metabolomic analysis shows that *dog1* enhances metabolic changes in the *brm-3*
201 background as many changes are only visible or more pronounced in the double *brm-3dog1-4*
202 mutant. In addition to untargeted analysis of metabolites, a targeted analysis of soluble sugars
203 and hormones was performed in the mature seeds of the mutants. This analysis showed that ABA
204 levels were slightly reduced in *brm-3* and *dog1-4* mutant seeds while double mutant seeds
205 showed intermediate levels of ABA, with no significant difference to either Col-0 or single
206 mutants (Supplementary Fig. S3A). The small effect on ABA suggests that phenotypic defects
207 observed in *brm-3* and double mutant are probably not driven through ABA. Similarly, analysis
208 of GA levels in dry seeds showed no significant difference for *brm-3* seeds and higher but not
209 significant levels for *dog1-4* and double mutant seeds (Supplementary Fig. S3B). Given the
210 published role of sugars in seed maturation, we also analyzed levels of sucrose, raffinose and
211 stachyose (Li *et al.*, 2017; Salvi *et al.*, 2022). Seeds of *brm-3* and *brm-3dog1-4* contained
212 significantly higher levels of raffinose and lower levels of sucrose, resulting in increased
213 RFO/sucrose ratio (Supplementary Fig. S4A, 4B, 4C). Likewise, stachyose levels were also
214 lower in seeds of the *brm-3* single and *brm-3dog1-4* double mutant (Supplementary Fig. S4D). In
215 contrast, seeds of *dog1-4* mutant did not show changes in sugar levels. These results suggest that
216 BRM is implicated in sugar level control in seeds but independently of DOG1 (Supplementary
217 Fig. S4).

218 In summary, our metabolomic analysis revealed that *brm-3* and *dog1-4* share some common
219 differentially enriched compounds compared to the wild type, while much more diverse families
220 of metabolites are differentially enriched in the double mutant, confirming the synergistic action
221 of BRM and DOG1 in seeds biology (Supplementary Fig. S1, Supplementary Table 1).
222 Interestingly, our data suggest the glutathione level is controlled by BRM in a DOG1 dependent
223 manner, as it was increased in *brm-3* mutant while in *dog1-4* and *brm-3dog1-4* double mutant
224 glutathione was less abundant compared to Col-0 WT seeds (Fig. 1F, 1E, Supplementary Fig.
225 S5).

226 **BRM regulates seed quality and physiology**

227 To assess the BRM and DOG1 effect on seed quality, we first checked the seed size in single and
228 double mutants (Fig. 2A, B and Supplementary Fig. S6A). The *brm-3* mutant seeds were 20%
229 bigger compared to the wild type and the *dog1-4* mutant, with an average size of 0.27, 0.21 and
230 0.23 mm² for *brm-3*, *dog1-4* and the wild type, respectively (Fig. 2B, Supplementary Fig. S6A).
231 The *brm-3* mutant seeds were also 25% heavier (p-value < 0.00095) compared to the wild type.
232 In addition, even though *brm-3dog1-4* seeds were not significantly larger than Col-0 WT seeds,
233 double mutant seeds were significantly heavier than Col-0 seeds (Supplementary Fig. S6D). In
234 addition, germination rate of *brm3* and *brm3dog1-4* double mutants in the presence of ABA was
235 similar to Col-0 WT seeds (Supplementary Fig. S6C). As previously reported for *brm-3* (Farrona
236 et al., 2007), *brm-3* and *brm-3dog1-4* mutants had significantly reduced seed yield while *dog1-4*
237 mutant did not show a difference compared to the wild type (Fig. 2C). Our data suggest that seed
238 quality measured by seed size, weight but not yield is affected by BRM in DOG1 dependent
239 manner.

240 Glutathione is one of the main antioxidants in seeds and its level decreases during seed ageing
241 (Ranganathan & Groot, 2023). Our metabolomic analysis showed changes in glutathione levels
242 prompting us to analyze the role of BRM in longevity. Seeds of *brm-3* mutant showed increased
243 longevity compared to the wild type (Supplementary Fig. S6B), as seen in the analysis of the
244 time required for 50% loss of viability (P₅₀, Fig. 2D). As published by Dekkers et al. 2016, we
245 observed that the P₅₀ of the *dog1-4* mutant was lower compared to the wild type, demonstrating a
246 role of DOG1 in enhancing longevity. Interestingly, the P₅₀ of the double mutant *brm-3dog1-4*
247 was only slightly higher than for the single *dog1-4* mutant. In addition, we performed a
248 germination analysis of 4-year-old naturally aged seeds of the tested mutants. This analysis
249 revealed a germination phenotype similar to that observed in artificially aged seeds: the *brm3*

250 mutant showed significantly higher germination rates compared to Col-0 WT seeds, but this
251 effect was suppressed in the *brm3dog1-4* double mutant (Supplementary Fig. S6E). This suggests
252 that BRM role in seed longevity is partially DOG1 dependent.

253 As we found BRM affects seed longevity, we were further interested in its effect on seed's vigor.
254 We analyzed salt sensitivity during germination of after-ripened seeds (Fig. 2E). After-ripened
255 seeds of *brm-3* showed no difference in germination in presence of 100mM NaCl compared to
256 Col-0. In contrast to what has been observed for freshly harvested stratified seeds, the *dog1-4*
257 mutant showed reduced germination when compared to Col-0 WT (Montez *et al.*, 2023). The
258 *brm-3dog1-4* double mutant behaved like the *dog1-4* single mutant suggesting that BRM is not
259 involved in salt-mediated germination delay (Fig. 2E). Given the role of DOG1 in dormancy, we
260 performed primary and secondary dormancy tests on the mutants. Primary dormancy was tested
261 by germination of freshly harvested seeds and secondary dormancy was analyzed on seeds pre-
262 treated with high temperature in the darkness (Footitt *et al.*, 2015; Krzyszton *et al.*, 2022). In
263 agreement with published results (Krzyszton *et al.*, 2022), we observed that the *DOG1* gene is
264 required for primary as well as secondary dormancy, as the *dog1-4* mutant showed nearly 100%
265 germination of both freshly harvested seeds and seeds induced into secondary dormancy. In
266 contrast, the *brm-3* mutant displayed a stronger secondary but unaffected primary dormancy
267 when compared to Col-0 WT seeds (Fig 2F, G), suggesting a specific function of BRM in
268 secondary dormancy regulation. Likewise for *brm-3*, stronger secondary seed dormancy was also
269 observed in *brm-5*, *3xbrd* and *swp73a*, other *SWI/SNF* subunit mutants (Supplementary Fig. S7,
270 S8A).

271 In summary, we showed that BRM is an important regulator of seed biology required for many
272 aspects of seed development and environmental sensing. Our data reveals a genetic requirement
273 of the functional *DOG1* gene for BRM-mediated control of seed longevity and secondary
274 dormancy. The lack of primary seed dormancy defects and stronger secondary seed dormancy
275 observed in *brm-3* and *brm-5* mutants is surprising, as primary and secondary dormancy levels
276 are usually correlated in Arabidopsis mutants (Buijs, 2020; Sajeev *et al.*, 2024).

277

278 **BRM binds to the *DOG1* 3' region and regulates *asDOG1* antisense expression**

279 Our genetic analyses suggested that BRM-mediated regulation of secondary dormancy requires
280 the *DOG1* gene. Previously, it has been shown that the *DOG1* gene 3' end is bound by BRM and
281 BRD in seedlings (Yu *et al.*, 2020, Yu *et al.*, 2021, Archacki *et al.*, 2016, Supplementary Fig.

282 S9A, S9B). To confirm BRM binding at the *DOG1* locus in seeds, we performed ChIP-qPCR
283 experiment using a transgenic line expressing BRM-GFP under a native promoter in the
284 background of *brm-1* null mutant (Jarończyk *et al.*, 2021). We observed BRM binding mostly
285 within exon 2 and exon 3 of the *DOG1* gene, matching the location of previously described by us
286 antisense lncRNA *DOG1* promoter (Fig. 3A). This suggests that BRM could control the *DOG1*
287 gene expression in seeds via *asDOG1* (Fedak *et al.*, 2016).

288 In non-dormant dry seeds, BRM was bound at exon 2 and exon 3 regions (*asDOG1* promoter),
289 similar to genome-wide ChIP data from Arabidopsis seedlings (Fig. 3B, Supplementary Fig. S9).
290 During SD induction, BRM was predominantly bound at exon 3 (Fig. 3B). This suggests that
291 secondary dormancy induction may lead to changes in the way BRM controls *DOG1* sense and
292 antisense expression. This is in agreement with our phenotypic analysis (Fig. 2G, Supplementary
293 Fig. S7) that demonstrated that *brm-3* seeds show an enhanced propensity to enter secondary
294 dormancy while seeds collected from *brm-3dog1-4* double mutant are unable to enter dormancy.

295 Next, we performed RT-qPCR analysis of *DOG1* gene expression in the Col-0 WT and selected
296 mutants during secondary dormancy induction. Upon imbibition at 4 hours, we observed a strong
297 *DOG1* mRNA reduction followed by a gradual rebuild of *DOG1* mRNA levels during secondary
298 dormancy induction (Fig. 3C). This is in agreement with previously published by us and others'
299 results (Buijs G. 2020; Krzyszton *et al.* 2022; Sajeev *et al.* 2024). Interestingly, we observed a
300 much stronger increase in *DOG1* mRNA levels in *brm-3* mutant (Fig 3C). To test if the observed
301 BRM role in *DOG1* expression regulation during secondary dormancy induction requires activity
302 of the whole BAS complex, we used a single *swp73a* and a triple *BRD1/2/13* (*3xbrd*) mutant that
303 both are components of BAS SWI/SNF complex (Guo *et al.*, 2022; Fu *et al.*, 2023). We observed
304 hyper activation of *DOG1* expression in *3xbrd* and *swp73a* mutant seeds (Fig. 3C,
305 Supplementary Fig. S8B) that was very similar to the one observed in *brm-3*. We also note a
306 stronger dormancy phenotype during secondary dormancy induction for *3xbrd* and *swp73a*
307 mutants (Supplementary Fig. S7, S8A). The observed upregulation of *DOG1* expression in the
308 *brm-3*, *swp73a* and *3xbrd* mutants suggests a previously unrecognized role for BRM and the
309 SWI/SNF BAS-complex in the suppression of *DOG1* expression during secondary dormancy
310 establishment. Gene expression analysis showed increase in the mRNA levels of the *BRM* and
311 *SWP73A* genes but not for *BRD1*, suggesting that the main SWI/SNF subunits are co-induced
312 with *DOG1* gene during secondary dormancy establishment. However, BRM expression was not
313 affected in *dog1-4* mutant compared to Col-0 WT seeds during induction (Supplementary Fig.

314 S10A). Thus, our genetic and RT-qPCR analyses suggested that BRM function upstream of the
315 *DOG1* gene.

316 In parallel to sense transcript expression during secondary dormancy induction, we analyzed
317 *asDOG1* transcript levels. Similarly, to sense transcript expression, we observed a gradual
318 accumulation of antisense transcript during dormancy induction (Fig. 3D). All *brm-3*, *swp73a*
319 and *3xbrd* mutants showed a clear reduction in the levels of *asDOG1* expression when compared
320 to the Col-0 seeds at later stages of dormancy induction (Fig. 3D, Supplementary Fig. S9C).
321 Together with BRM binding at *DOG1* 3' end this suggests that BRM directly regulates *asDOG1*
322 transcription. To test this possibility, we used the p_{ASDOG1} promoter-driven IRES-LUC reporter
323 line and crossed it with the *brm-3* mutant. RT-qPCR using LUC primers showed significant
324 downregulation of *LUC* transcript in *brm-3*, suggesting that BRM directly regulates *asDOG1*
325 promoter activity (Fig. 3F).

326

327 **BRM regulation of *DOG1* gene expression requires *asDOG1***

328 Observed by us direct regulation of *DOG1* antisense expression by BRM and the lack of BRM
329 binding to canonical *DOG1* promoter suggested a model where BRM regulates *DOG1* sense
330 expression through *DOG1* antisense. To test this model, we first asked if BRM can regulate
331 *DOG1* expression in the absence of *asDOG1*. We used a previously published (Fedak *et al.*,
332 2016) transgenic truncated *DOG1* gene ($p_{DOG1shDOG1::LUC}$) with an antisense promoter deleted
333 and crossed it to a *brm-3* mutant (Fig. 3E). Importantly, no significant differences were observed
334 between Col-0 and *brm-3* suggesting that BRM is unable to regulate the *DOG1* gene expression
335 when the *DOG1* 3' region is removed. Surprisingly, $p_{DOG1shDOG1::LUC}$ did not show the
336 induction of expression that we observed for endogenous sense mRNA.

337 Therefore, the inability of BRM to regulate *DOG1* gene with antisense deleted ($p_{senseDOG1}$ -
338 *LUC*), together with the fact that in *brm-3* mutant p_{ASDOG1} activity is suppressed, suggest that
339 BRM acts through antisense. The fact that $p_{senseDOG1-LUC}$ transgene did not recapitulate
340 endogenous *DOG1* sense expression inductions suggest that some of the elements required for
341 *DOG1* induction upon secondary dormancy induction are located in regions deleted in the
342 construct.

343 To test this possibility, we took advantage of a set of TATA mutations shown by us previously to
344 greatly reduce *asDOG1* transcript expression (Yatusevich *et al.*, 2017). We engineered these
345 mutations in an antisense promoter of the *DOG1* genomic reporter construct creating *LUC*-

346 *DOG1-deltaTATA* transgenic lines. RT-qPCR analysis using primers that amplify only
347 transgene-originating *DOG1* mRNA showed that removal of antisense transcription indeed
348 resulted in strong upregulation of *DOG1* sense transcript at early stages of dormancy induction
349 (Fig. 3G, Supplementary Fig. S11A, S11B). Together the transgenes analysis shows that BRM
350 requires *asDOG1* to control *DOG1* expression during secondary dormancy induction and that
351 *asDOG1* acts as negative regulator of *DOG1* expression during secondary dormancy
352 establishment. Similar to *brm-3* and *brm-5* mutants, transgenic *LUC-DOG1* lines carrying
353 dTATA mutations showed stronger secondary seed dormancy compared to WT *LUC-DOG1*
354 lines, confirming *asDOG1* acts as a negative regulator of *DOG1* expression during secondary
355 dormancy (Supplementary Fig. S11C).

356 BRM is part of the SWI/SNF complex and our data show that both BRM and another SWI/SNF
357 complex subunits - BRDs are implicated in seed secondary dormancy control through *asDOG1*
358 antisense transcript promoter regulation. SWI/SNF is a chromatin remodeling complex that
359 utilizes ATP to remodel chromatin at target loci (Mashtalir *et al.*, 2018). To test if BRM-
360 mediated regulation of *DOG1* sense expression through *asDOG1* is accompanied by DNA
361 accessibility changes, we performed FAIRE (Formaldehyde-Assisted Isolation of Regulatory
362 Elements) during secondary dormancy induction (Omidbakhshfard *et al.*, 2014). On the third day
363 of secondary dormancy induction, *brm-3* showed a marked increase in DNA accessibility using
364 FAIRE at the end of exon 2 compared to dry seeds (Fig. 4A, 4B). This increase was even more
365 pronounced in the last intron and exon 3 of the *DOG1* region on the 5th day of induction,
366 centering around the *DOG1* antisense promoter region (Supplementary Fig. S8D). This region
367 colocalized with the BRM binding site identified in ChIP experiments (Fig. 3A, B; Fig. 4A, B;
368 Supplementary Fig. S8C, S8D). In agreement with BRM involvement in *DOG1* regulation during
369 secondary dormancy, the FAIRE experiment in dry seeds failed to detect a localized increase at
370 *DOG1* 3' end in *brm-3* compared to Col-0 WT dry seeds (Fig. 4A). Thus, this suggests that
371 during secondary dormancy induction, BRM is directly bound at *DOG1* 3' end and locally
372 remodels chromatin presumably to regulate *asDOG1* expression. This is consistent with the
373 *asDOG1* requirement for BRM's ability to suppress *DOG1* gene expression during secondary
374 dormancy induction.

375 **BRM affects *DOG1* splicing and polyadenylation**

376 To gain a deeper understanding of *DOG1* regulation by BRM, we analyzed the misregulation of
377 *DOG1* splicing and polyadenylation in *bmr-3* seeds during the induction of secondary dormancy.

378 Our RT-qPCR analysis examined early time points (2- and 4-days post-induction) for splicing
 379 and up to 14 days post-induction for polyadenylation. We detected increased levels of the short
 380 proximally polyadenylated *DOG1* mRNA (*shDOG1*), but not the long form (*lgDOG1*), during
 381 secondary dormancy induction in *brm-3* (Fig. 4C, 4D). We also found a significant increase in β
 382 (beta) and γ (gamma) *DOG1* mRNA splicing forms in *brm3* mutants compared to Col-0 seeds
 383 (Fig. 4E-H). Increased β , γ and *shDOG1* were not only observed in *brm-3* but also in *3xbrd*
 384 mutant, suggesting that they are a result of BRM activity linked to SWI/SNF complex. The
 385 increase in β , γ and *shDOG1* mRNA is consistent with the observed stronger *brm-3* mutant
 386 secondary seed dormancy phenotype as *shDOG1* has been reported to be the predominant *DOG1*
 387 isoform that can complement the *DOG1* mutant phenotype and β and γ mRNA isoforms lead to
 388 production of the same protein as encoded by *shDOG1*. Interestingly, in the *ntr1* mutant, known
 389 as a spliceosome disassembly factor (Dolata J *et al.*, 2015), we observed a significant reduction
 390 in *DOG1* mRNA splicing forms, while other β , γ and δ splicing forms showed similar kinetics
 391 to one observed in Col-0 WT (Supplementary Fig. S15). The differential effect of *brm-3* and *ntr1*
 392 on *DOG1* splicing suggest that BRM does not control *DOG1* splicing through NTR1.

393

394 DISCUSSION

395 BRM containing SWI/SNF complex controls seed physiological quality

396 We show that *brm-3* mutant exhibit multiple seed-related phenotypes, including enlarged seed
 397 size, reduced seed yield, increased seed longevity and enhanced secondary dormancy induction
 398 but no change in primary dormancy or germination in the presence of salt (Fig. 2, Supplementary
 399 Fig. S14). Given the central role of the *DOG1* gene in seed biology as well as BRM binding to
 400 *DOG1* locus, we tested the interplay of *BRM* and *DOG1* genes in seeds. We found that some of
 401 the *brm-3* mutant phenotypes are genetically dependent on *DOG1* gene as a double mutant of
 402 *brm-3dog1-4* shows a reversal of the longevity and secondary dormancy phenotypes (Fig. 2).
 403 Transcriptomic analysis in dry seeds showed that around 20% of genes misregulated in *brm-3* are
 404 *DOG1* gene-dependent as *dog1-4* mutation can partially or fully suppress the *brm* mutation effect
 405 on their expression in the *brm-3dog1-4* double mutant (Fig. 1D). In addition, we observed a
 406 pronounced misregulation of gene expression in the double *brm-3dog1-4* double mutant (Fig.
 407 1A) which suggests a synergistic function in the case of the majority of affected genes.

408 Longevity and metabolite accumulation

409 GO terms analysis among differentially regulated genes suggested changes in genes involved in
410 the biosynthesis of metabolites known to be important in seed biology (Supplementary Table 1)
411 that were mostly consistent with changes observed in seed metabolome analysis (Supplementary
412 Fig. S1A, 1B). RNA-seq data showed that genes related to glutathione metabolism were enriched
413 among genes downregulated in *brm-3dog1-4* double and *dog1-4* single mutant and upregulated in
414 single *brm-3* mutant (Supplementary Fig. S2, S5). This is consistent with our metabolomic
415 analysis that showed an increase in *brm-3* and lower levels of glutathione in *dog1-4* and *brm-3*
416 *3dog1-4* mutants (Fig. 1F, Supplementary Fig. S5). Given the published link between glutathione
417 level, dormancy and longevity in Arabidopsis (Cairns *et al.*, 2006; Nguyen *et al.*, 2015;
418 Koramutla *et al.*, 2021), we note that the observed changes in glutathione level are probably
419 responsible for the observed *DOG1* gene-dependent partial increase in longevity of *brm-3*
420 mutant. This observation is corroborated by the suggested previously positive role of *DOG1* in
421 longevity based on analysis of natural variation and *DOG1* NIL line analysis (Nguyen *et al.*,
422 2012).

423 Changes in soluble sugar contents have been suggested to be involved in germination and
424 longevity regulation (He *et al.*, 2016). In legume species, a correlation between lower seed
425 storability and a lower ratio between RFO and sucrose has been reported (Pereira Lima *et al.*,
426 2017). While in Arabidopsis, this correlation remains unclear, as an increase in the RFO/sucrose
427 ratio was not found to be correlated with seed vigor (Bentsink *et al.*, 2000; Li *et al.*, 2017). We
428 found a significant decrease in RFO/sucrose ratio in both single *dog1-4*, *brm-3* and double
429 mutants (Supplementary Fig. S4B). However, there is no significant difference in this ratio
430 between *dog1-4* and *brm-3* mutants, despite the difference in seed longevity between them. Thus,
431 our data suggest that in Arabidopsis, there might be no direct link between RFO and seed
432 longevity. However, it is interesting to further investigate galactinol contents as it has been linked
433 to seed biology and has not been measured by us (De Souza Vidigal *et al.*, 2016).

434 In addition, in dry *brm-3* mutant seeds, we observed significant alterations in various classes of
435 tryptophan-derived metabolites, including auxin, camalexin, and indole-glucosinolates. The
436 deregulation of genes involved in the tryptophan-derived metabolite pathways (such as *MYB34*,
437 *MYB51*, *MYB122*, *NITs*, *ARFs*, *CYP79B3* etc.) in the *brm* mutant may contribute to the observed
438 auxin-related phenotypes and reduced seed yield of *brm-3* (Supplementary Fig. S2B). While
439 camalexin and indole-glucosinolates are recognized as plant defensive secondary compounds
440 against pathogens and herbivores (Stotz *et al.*, 2011; Nguyen *et al.*, 2020), their specific
441 biological roles in seeds dormancy remain to be fully elucidated.

442 **The role of BRM in glutathione accumulation in seed is *DOG1*-dependent**

443 Glutathione is an important player in redox signaling and is involved in protection against
444 excessive oxidation in multiple plant tissues (Mhamdi *et al.*, 2010). Accumulation of oxidative
445 damage during dry seed storage is probably the most important factor behind deterioration of
446 seed quality and eventually loss of viability determining seed longevity (Kumar *et al.*, 2015). Our
447 transcriptomic analysis showed that genes related to glutathione metabolism were misregulated in
448 *brm-3* mutant in the opposite direction to changes observed in *dog1-4* mutant, including *GPXI*
449 and *GPX6* that are responsible for glutathione biosynthesis. We also observed multiple other
450 misregulated genes in different pathways related to glutathione synthesis, degradation and
451 recycling. Genes coding for GLUTATHIONE S-TRANSFERASEs: GSTU9, GSTU10, GSTU11,
452 GSTU12 and GSTU19 were significantly up-regulated (FDR < 0.05, FC > 2) in mature seeds of
453 *brm-3* mutant compared to Col-0 WT seeds (Fig. 1F, Supplementary Fig. S2, S5). No consistent
454 change of the transcript levels of these genes were observed in *dog1-4* seeds.

455 In agreement with the observed deregulation of glutathione-related transcripts, we observed a
456 higher level of glutathione in the *brm-3* mutant, and depletion in *dog1-4* and double mutant
457 compared to Col-0. Those results are concordant with the reduced longevity in both *dog1-4* and
458 double mutant, and the increased longevity of the *brm-3* mutant.

459 **ABA and GA hormonal signaling in *brm-3* mutant seeds during SD**

460 Our analysis of hormone levels in dry seeds revealed relatively minor differences in the single
461 mutants *brm-3* and *dog1-4* regarding GA and auxin content (Supplementary Fig. S3B, S3C).
462 Interestingly, we observed a significantly elevated auxin level in the *brm-3 dog1-4* double
463 mutant (Supplementary Fig. S2C), correlating with increased expression of auxin pathway genes
464 (Supplementary Fig. S7B). A slight reduction in ABA levels was detected in *dog1-4* and slightly
465 in the double mutant (Supplementary Fig. S3A). Members of the SWITCH2 (SWI2)/SNF2
466 chromatin-remodeling complexes play a role in seed germination under ABA treatment.
467 BRAHMA (BRM) directly suppresses the expression of ABI5 and, consequently, the *brm-3*
468 mutant exhibits increased ABA sensitivity during seed germination (Han *et al.*, 2012). The role
469 of ABA and its signaling pathway in seed biology has been extensively studied, including its role
470 in secondary seed dormancy establishment (Auge *et al.*, 2015; Ibarra *et al.*, 2016).

471 In agreement with published results, we have previously reported that quadruple *nced2469*
472 mutant failed to enter into secondary dormancy (Lefebvre *et al.*, 2006; Krzyszton *et al.*, 2022).
473 Here, we show that *nced2469* shows no defect in *DOG1* expression during secondary dormancy

474 induction when compared to Col-0 seeds (Supplementary Fig.S10B). Also, analysis of the
475 expression of genes related to ABA biosynthesis and catabolism (*NCED4/5* and *CYP707A2*)
476 showed only minor fluctuations during secondary dormancy induction in Col-0 seeds and no
477 major differences when compared to *brm-3* or *dog1-4* mutants (Supplementary Fig. S12A,
478 S13A). In contrast, we observed a strong induction of *RGL1*, *RGL2* and *GAI* genes - known
479 negative regulators of the GA pathway, during secondary dormancy induction. Interestingly
480 *RGL1* and *RGL2* but not *GAI* showed strong upregulation in *brm-3* mutant when compared to
481 WT seeds during dormancy induction (Supplementary Fig. S12B). In contrast, in *dog1-4* mutant
482 only *RGL1* and *GAI* genes were induced (Supplementary Fig. S13B). While we did not analyze
483 the levels of gibberellins during secondary dormancy induction, this may suggest a role of GA
484 catabolism genes rather than ABA in enhanced secondary dormancy induction in *brm-3* (Ibarra
485 *et al.*, 2016; Chang *et al.*, 2018) and required functional *DOG1*.

486 **BRM controls secondary seed dormancy through *DOG1* antisense**

487 In agreement with the genetic interplay between *BRM* and *DOG1* genes, we detected direct BRM
488 binding to exon 2 and exon 3 of the *DOG1* gene in dry seeds. Interestingly, during secondary
489 dormancy induction, BRM binding increased towards the 3' end of the *DOG1* locus (Fig. 3A, B).
490 Together with the observed deregulation of the *DOG1* gene expression and changes in chromatin
491 accessibility, this suggests that BRM controls secondary dormancy directly through *DOG1*.
492 Primary and secondary dormancy are intrinsically linked and multiple factors including *DOG1*,
493 *AFP2*, *ABI5* and *ABI3* have been shown to affect both primary and secondary dormancy (Han *et al.*,
494 2012; Ibarra *et al.*, 2016; Chang *et al.*, 2018). Here, we show that BRM is specifically
495 implicated in secondary but not primary dormancy control. To the best of our knowledge, this is
496 the first example of where a factor is required only for secondary but not primary seed dormancy.

497 *DOG1* is a known positive regulator of dormancy (Bentsink *et al.*, 2006). Here we show that
498 during secondary dormancy induction, sense *DOG1* transcript is induced (Fig. 3C). This is in
499 agreement with published by us and others requirement of functional *DOG1* gene for secondary
500 dormancy establishment (Ibarra *et al.*, 2016; Krzyszton *et al.*, 2022; Sajeev *et al.*, 2024). Our data
501 show that in *brm-3* seeds *DOG1* transcript is upregulated while *asDOG1* is downregulated during
502 secondary dormancy induction, when compared to Col-0 (Fig. 3C, 3D). We also observe BRM
503 binding to *DOG1* 3'end region, and that BRM regulates *asDOG1* but not *DOG1* sense promoter
504 activity during secondary dormancy establishment (Fig. 3). Supporting a direct role of BRM in
505 control of *asDOG1* we observed increased DNA accessibility at *asDOG1* promoter region of the

506 *DOG1* locus in *brm-3* mutant during secondary dormancy establishment (Fig. 4A). Interestingly,
507 BRM binds to the 3' end region of selected differentially expressed genes (DEGs) involved in
508 ABA and GA pathways (such as *RGL3*, *NCED4*, *CYP707A1* etc.) (Supplementary Table 2).

509 Previous research has shown that *asDOG1* is a negative regulator of *DOG1* expression, as its
510 deletion results in high *DOG1* expression (Fedak *et al.*, 2016, Yatusевич *et al.*, 2017). BRM
511 appears to positively control antisense, thus also negatively regulating *DOG1* gene expression
512 (Fig. 4, 5). The mechanism of *DOG1* silencing by its antisense, aka *IGOD*, is not yet fully
513 understood. We hypothesize that during secondary dormancy establishment, BRM indirectly
514 limits *DOG1* induction by enhancing *asDOG1* expression (Fig. 3D). In agreement, we show that
515 mutation of TATA boxes located in the antisense promoter region resulted in much stronger
516 *DOG1* upregulation compared to not mutated *DOG1* transgene and, in agreement, enhanced
517 secondary dormancy phenotype in seeds. Our model suggests that observed by us in Col-0
518 upregulation of *asDOG1* during secondary dormancy induction serves to limit *DOG1* induction
519 attenuating dormancy strength. In contrast to BRM function in secondary dormancy, both RNA-
520 seq and RT-qPCR showed no major differences in *DOG1* sense and antisense transcripts levels
521 between Col-0 and *brm-3* mutant in dry seeds. This agrees with the observed lack of primary
522 dormancy defects in *brm-3* as well as in *3xbrd* and *swp73a* mutants (Fig. 2F, Supplementary Fig.
523 S14).

524 Notably, the introduction of triple *3xbrd* mutation into the *brm-1* knockout mutant background
525 did not enhance the *brm-1* phenotype, confirming the conclusion that BRD subunits operate
526 within the same complex as BRM (Stachula *et al.*, 2023). Also, here we show that *3xbrd* and
527 *swp73a* display similar *DOG1* expression changes to *brm-3* mutant consistent with BRM
528 operating as part of BAS SWI/SNF complex in controlling *DOG1* expression (Fig. 3,
529 Supplementary Fig. S9).

530 Thus, we propose a model where BRM-containing the SWI/SNF complex binds to the *DOG1*
531 3'end region and in response to secondary dormancy-inducing conditions remodels nucleosomes
532 which activate *asDOG1* antisense promoter (Fig 5). This leads to *asDOG1* transcript expression
533 that limits the activation of *DOG1* and subsequently to a strong dormancy establishment.
534 Surprisingly, analysis of *p_{sense}DOG1-LUC* transgene that lacks a function *DOG1* antisense
535 transcript in seeds showed that *DOG1* 5'region is insufficient to support *DOG1* expression
536 upregulation in response to secondary dormancy induction. This suggests that in addition to
537 *DOG1* antisense that limits the full activation of *DOG1* expression, the *DOG1* 3'end region

538 contains unknown positive regulators responsible for secondary dormancy-mediated *DOG1*
539 expression induction.

540 Analysis of *DOG1* splicing and polyadenylation during secondary seed dormancy induction in
541 Col-0 WT, *brm3* showed increased levels of β and γ alternatively spliced mRNA as well as
542 increased levels of *shDOG1* resulting from selection of proximal termination site (Fig. 4F, 4G).
543 Whereas in the *ntr1* mutant, we observed predominantly changes in α and not significantly in β
544 *DOG1* mRNA splicing forms compared to Col-0 WT seeds (Supplementary Fig. S15). Given that
545 our work implicated NTR1 in splicing control through Pol II speed on *DOG1* we speculate that
546 defects observed in *brm-3* are unlikely to results from NTR1 dependent splicing defects or direct
547 Pol II speed regulation. One possibility is that changes in *DOG1* splicing and termination site
548 selection observed in *brm-3* and *3xbrd* result from defects in antisense expression in these
549 mutants. The proximity of *DOG1* alternative splice sites - proximal termination site and antisense
550 promoter make deletional confirmation of this hypothesis difficult, if possible. We, however,
551 showed that BRM regulates the *DOG1* antisense promoter in seeds in the absence of sense
552 promoter driving *DOG1* alternative splicing or proximal termination site selection.

553 In summary, our work explores the functions of the BRM-containing SWI/SNF complex in seed
554 biology. We observe that BRM is required for multiple aspects of seed physiology as
555 underpinned by metabolomic and transcriptomic analysis. We show that BRM controls some of
556 the seed-related phenotypes including longevity and secondary dormancy regulation through the
557 *DOG1* gene. Our analysis demonstrates that in response to environmental signals triggering
558 secondary dormancy induction BRM containing SWI/SNF complex controls *DOG1* expression
559 through *DOG1* antisense.

560

561 **Materials and Methods**

562 **Plant Material and Growth Conditions**

563 *Arabidopsis thaliana* plants were grown in pots with mixed coconut and normal soil in a
564 greenhouse with a long-day photoperiod (16-h light/8-h dark) at 22°C/18°C. After harvest, seeds
565 were stored in paper bags at room temperature. Ecotype Col-0 plants were used as a wild type
566 (WT). The *brm-3* (SALK_088462) and *dog1- 4* (SM_3_20886) mutants were obtained from the
567 Nottingham Arabidopsis Stock Centre (NASC) and are described in (Farrona et al., 2007; Fedak
568 et al., 2016). Transgenic reporter lines: genomic *LUC-DOG1dTATA*, *asDOG1dTATA-LUC*,

569 *senseDOG1-LUC*, *asDOG1-LUC*, and *genomicLUC-DOG1* were generated and characterized
570 previously (Fedak et al., 2016; Yatusевич et al., 2017). The *brm-5*, *swp73a* (SM_3_30546),
571 *3xbrd*, *ntr-1*, *4xnced* and *brm-1/BRM-GFP* lines were described previously (Tang et al., 2008;
572 Dolata et al., 2015; Sacharowski et al., 2015; Jarończyk et al., 2021; Krzyszton et al., 2022). The
573 double mutants: *brm-3dog1-4*; *brm-3p_{sense}DOG1-LUC*; *brm-3p_{AS}DOG1-LUC*; *brm-3genomic*
574 *LUC-DOG1dTATA*; *brm-3p_{AS}DOG1dTATA-LUC* were generated by crossings and homozygous
575 plants were identified using *brm-3* T-DNA insertion primers described in Jarończyk et al., 2021.

576 For salt stress, sterilized after-ripened seeds were sown on agar plates supplemented with 100mM
577 NaCl. After sowing, plates were taped, wrapped with silver foil, and kept for stratification for 3
578 days at 4°C. Then plates were unwrapped from the silver foil and transferred to the growth
579 chamber under long-day conditions (16h light/8h dark) to check the germination rate (Montez et
580 al., 2023).

581 **Seed Longevity Measurement**

582 To perform artificial ageing, mature post-harvested *Arabidopsis* seeds were stored in the darkness
583 at 35°C in hermetically closed containers with saturated NaCl (75% of relative humidity). 50
584 seeds per each biological replica were imbibed on blue paper (Anchor) plates after different
585 storage times (0, 7, 14, 21, 28, 35, 42, 49, 56 days) and placed in a phytotron at 22°C/long day
586 photoperiod. The final germination percentage was counted after 10 days. P50 was determined as
587 the time after which seeds lost 50% of their germination capacity (Zinsmeister et al., 2020).

588 **Seed primary dormancy assay**

589 Freshly harvested seeds were sown on plates with water-soaked blue paper (Anchor) and sealed
590 with tape. Plates with the seeds were put in the growth chamber under long-day conditions (16
591 hours light/8 hours dark) at 22°C/18°C. The germination rate was scored every day until 100%
592 germination was observed. Control plates were initially stratified for 3 days at 4°C to break seed
593 dormancy and to ensure that the seeds were not dead.

594 **Seed secondary dormancy assay**

595 Seeds stored for at least 3 months that showed full loss of primary dormancy were used for
596 secondary dormancy induction. Seeds were sown on water-soaked blue paper plates, sealed and
597 kept in the dark. Plates were incubated at 30°C for 4 hours, 1, 3, 5, 7, 10 or 14 days. After high
598 incubation, the plates were transferred to the growth chamber at 22°C under long-day conditions.

599 Seed germination was assayed after 4 and 7 days. The control plates were placed in a phytotron
600 immediately after sowing the seeds, without a dormancy induction.

601 **RNA extraction, cDNA synthesis and RT–qPCR analysis**

602 RNA extraction from seeds was performed using the phenol-chloroform protocol. The frozen
603 seeds were ground to a powder using an electric drill and then mixed with 600 µl of RNA
604 extraction buffer (100 mM Tris pH 8.5, 5 mM EDTA pH 8.0, 100 mM NaCl, 0.5% SDS, 1% β-
605 mercaptoethanol). Afterwards, samples were centrifuged for 5 min at 14,000 g at 4°C. The
606 supernatant was transferred to new tubes and 250 µl of chloroform was added and samples were
607 shaken at room temperature (RT) for 15 min. Then 250 µl of phenol was added and samples were
608 shaken for a further 15 min and centrifuged for 10 min at 14,000 g at 4°C. Then, 550 µl of the
609 aqueous layer was transferred to new tubes and mixed with 550 µl of phenol–chloroform–
610 isoamyl alcohol 25:24:1. Samples were shaken for 10 min at RT and centrifuged for 10 min at
611 14,000 g at 4°C. Then, 500 µl of supernatant after transferring to new tubes was mixed with 50 µl
612 of 3 M sodium acetate and 400 µl of pure ice-cold isopropanol and incubated for 15 min at RT.
613 After the incubation, samples were centrifuged for 30 min at 14,000 g at 4°C. Finally, the RNA
614 pellet was washed in 1 ml of 80% ethanol, dried and resuspended in Milli-Q water. DNase
615 treatment of RNA samples was performed using a TURBO DNA-free™ Kit (ThermoFisher
616 Scientific), according to the manufacturer’s protocol. DNase treatment effectiveness was checked
617 by PCR with pp2A primers. Reverse transcription of RNA was performed using a RevertAid
618 First Strand cDNA Synthesis (ThermoFisher Scientific) or RevM First Strand cDNA Synthesis
619 (KleverLab) kits according to the manufacturer’s protocol. Two types of cDNA synthesis were
620 performed: using 1,000 ng of RNA and oligo(dT) primers for *DOG1* analysis and gene-specific
621 synthesis for *asDOG1* analysis using 2,500 ng of RNA and primers with overhangs as described
622 (Fedak *et al.*, 2016). qPCR was performed with SYBR Green mix and specific primers for PCR
623 amplification and with using LightCycler 480 real-time system (Roche). The sequences of all
624 primers are published previously (Cyrek *et al.*, 2016; Fedak *et al.*, 2016) and provided in the
625 Supplementary Table 2. RT–qPCR results were normalized to the expression level of the *UBC21*
626 (*AT5G25760*) gene.

627 **RNA-sequencing and data analysis**

628 3’RNA-seq and data analysis were performed as described previously using 500 ng of total RNA
629 as starting material (Krzyszton *et al.*, 2022).

630 Chromatin Immunoprecipitation (ChIP)

631 Chromatin was isolated from dry, non-dormant mature seeds and after 1, 3 and 5 days of
632 secondary dormancy induction for WT and *brm-1/BRM-GFP* lines (Jarończyk *et al.*, 2021). ChIP
633 was performed as described previously (Kowalczyk, 2017) with some modifications. The 60mg
634 of frozen seeds were ground to a powder using a pestle and mortar and suspended in 10ml of MC
635 buffer (0.1M sucrose; 10mM sodium phosphate pH 7; 50mM NaCl). Then 37% formaldehyde
636 was added to the final concentration of 1% and samples were mixed softly on a rotating wheel for
637 10 min at 4°C. After mixing, 625µl of 2M glycine was added and samples were rotated for
638 another 10 min. Then the samples were filtered through a double layer of Miracloth Quick
639 Filtration Material, and centrifuged for 10 min at 1500xg at 4°C. After centrifugation, samples
640 were resuspended in 5ml of Honda buffer (0.44M sucrose; 1.25% Ficoll; 2.5% Dextran T40;
641 20mM HEPES-KOH pH 7.4; 0.5M EDTA; 0.5% Triton X-100; 10mM β-Mercaptoethanol and
642 freshly added 0.0005M PMSF and 1×Complete EDTA-free protease inhibitor) and spun for
643 10min at 1800xg at 4°C. The nuclear pellet was resuspended in 500µl ChIP Lysis/sonication
644 buffer (50mM HEPES-KOH pH 7.4; 150mM NaCl; 1mM EDTA; 1% Triton X- 100; 0.8% SDS;
645 10mM β-Mercaptoethanol and freshly added 0.0005M PMSF and 1×Complete EDTA-free
646 protease inhibitor) and sonicated twice 30sec-ON/30s-OFF for 25min using Bioruptor Sonication
647 System (Diagenode). 1/10 of each sample was saved as input control and 20µl for sonication
648 control. Sonication efficiency was verified by running de-crosslinked samples on 1% agarose gel.
649 GFP-Trap® Agarose beads were prepared according to the manufacturer's protocol (Chromotek).
650 The lysates of sonicated samples were added to equilibrated beads and placed on a rotating wheel
651 in a cold room for 2-4 hours. After incubation, beads were centrifuged for 2500 x g for 5min at
652 4°C and washed twice for 5min with 1ml of low salt wash buffer (150mM NaCl; 1% Triton X-
653 100; 2mM EDTA; 20mM Tris pH 8.0; 0.1% SDS). Then beads were washed for 5min with 1ml
654 of high salt wash buffer (500mM NaCl; 1% Triton X-100; 2mM EDTA; 20mM Tris pH 8.0;
655 0.1% SDS) and centrifuged for 2500 x g for 5min at 4°C. Then 500 µl of
656 phenol:chloroform:isoamyl alcohol mixture (25:24:1; pH 8.0) were added and the samples were
657 shaken for 10 min at 22°C. After centrifugation for 10 min at 14,000 g the upper aqueous layers
658 were collected and 0,1 volume of 3M sodium acetate (pH 5.2), 1 µl of glycogen (ThermoFisher
659 Scientific), and 1 ml 96% ethanol were added. The mixed samples were held at -80°C for >1
660 hour and then centrifuged for 30 min at 14,000 g at room temperature. The pellets were washed
661 with cold 70% ethanol, air-dried and suspended in water. For the quantification of DNA
662 fragments, samples were tested by qPCR. The sequences of all primers are given in the
663 Supplementary Table 2 or published by (Dolata *et al.*, 2015).

664 **Formaldehyde-assisted isolation of regulatory DNA elements (FAIRE)**

665 The FAIRE method was performed according to the published protocol (Omidbakhshfard *et al.*,
666 2014) with minor modifications. For nuclei isolation, 100 mg of the dry and secondary
667 dormancy-induced seeds of *Col-0* and *brm-3* were used. Chromatin was sheared by sonication
668 and the sonication efficiency was checked by electrophoresis in agarose gel as previously
669 described for the ChIP protocol. To separate NDR (nucleosome-depleted regions), the sheared
670 chromatin DNA was extracted by PCI (phenol:chloroform:isopropanol) method. The enrichment
671 was assessed by qPCR using primers indicated in Supplementary Table 2. Calculations were
672 performed using the $\Delta\Delta C_t$ method with normalization of a crosslinked sample (FAIRE) to non-
673 crosslinked sample (UN-FAIRE) as described in Omidbakhshfard *et al.*, 2014 and then to *PP2A* –
674 AT1G13320 (Supplementary Table 2) as an internal control.

675 **METABOLOME ANALYSIS**

676 **Sample preparation**

677 Mature post-harvested seeds (50 mg) in biological triplicates were ground with metal beads for
678 2x 90s on a Tissue Lyser (Qiagen) at 30 Hz in 1.5 ml of cold (-20°C) methanol spiked with an
679 internal standard of deuterium labelled abscisic acid (2H_6 ABA, 0.2 μ gg/ml). Samples were
680 shaken for 10 minutes at RT, and centrifuged for 5 minutes at 13,000 rpm, RT. The supernatant
681 was transferred to a glass vial and the extract was dried with a SpeedVac concentrator (Savant
682 SPD121P, ThermoFisher Scientific) at RT. The pellets were extracted twice with 1.5 ml
683 methanol, shaken, centrifuged and collected in the same glass vial to be evaporated. After this,
684 dry samples were solubilized in 100 μ l of methanol.

685 **Non-targeted metabolites analysis**

686 Extracts were analyzed by liquid chromatography coupled to high-resolution mass spectrometry
687 (LC-HRMS) using an UltiMate 3000 UHPLC system (ThermoFisher Scientific) coupled to the
688 ImpactII (Bruker) high-resolution Quadrupole Time-of-Flight (QTOF) mass spectrometry
689 according to Villette *et al.* (2018) and Graindorge *et al.* (2022). Chromatographic separation was
690 performed on an Acquity UPLC $\text{\textcircled{R}}$ HSS T3 C18 column (2.1 \times 100 mm, 1.8 μ m, Waters) coupled
691 to an Acquity UPLC HSS T3 C18 pre-column (2.1 \times 5 mm, 1.8 μ m, Waters) using a gradient of
692 solvents A (H₂O, 0.1% formic acid) and B (methanol, 0.1% formic acid). Chromatography was
693 carried out at 35°C, at a flux of 0.3 ml min⁻¹, starting with 5% B for 2 min, reaching 100% B at
694 10 min, holding 100% B for 3 min and coming back to 5% B in 2 min (run time 15 min).

695 Samples were kept at 4 °C, 5 µL were injected in full loop mode with a washing step after
696 sample injection with 150µL of wash solution (H₂O/MeOH, 90/10, v/v). The spectrometer was
697 equipped with an electrospray ionization (ESI) source and operated in positive and negative ion
698 modes on a mass range from 20 to 1000 Da with a spectra rate of 8 Hz in Auto MS/MS
699 fragmentation mode. The end plate offset was set at 500 V, the capillary voltage set at 2.5 kV,
700 the nebulizer at 29 psi, the dry gas at 8 l min⁻¹, and the dry temperature of 200°C. The transfer
701 time was set at 20–70 µs (positive mode) and 40.8–143 µs (negative mode) and the MS/MS
702 collision energy was at 80–120% with a timing of 50–50% for both parameters. The MS/MS
703 cycle time was set to 3 s, the absolute threshold to 816 cts, and active exclusion was used with an
704 exclusion threshold at 3 spectra, release after 1 min, and the precursor ion was reconsidered if
705 the ratio current intensity/previous intensity was higher than 5. A calibration segment was
706 included at the beginning of the runs allowing the injection of a calibration solution from 0.05 to
707 0.25 min. The calibration solution used was a fresh mix of 50 mL isopropanol/water (50/50, v/v),
708 500 µL NaOH 1M, 75 µL acetic acid, and 25 µL formic acid. The spectrometer was calibrated on
709 the [M+H]⁺/[M-H]⁻ form of reference ions (57 masses from m/z 22.9892 to m/z 990.9196 in
710 positive mode; 49 masses from m/z 44.9971 to m/z 996.8221 in negative mode) in high-
711 precision calibration (HPC) mode with a standard deviation below 1 ppm before the injections
712 for each polarity mode, and re-calibration of each raw data was performed after injection using
713 the calibration segment. Molecular features were processed with MetaboScape version 4.0
714 (Bruker, Bremen, Germany). Molecular features were considered and grouped into buckets
715 containing one or several adducts and isotopes from the detected ions with their retention time
716 and MS/MS information when available. The parameters used for bucketing are a minimum
717 intensity threshold of 10,000 (positive mode) or 1,000 (negative mode), a minimum peak length
718 of 3 spectra, a signal-to-noise ratio (S/N) of 3, and a correlation coefficient threshold set at 0.8.
719 The [M+H]⁺, [M+Na]⁺, [M+K]⁺, and [M+NH₄]⁺ ions (positive mode); [M-H]⁻ and [M+Cl]⁻
720 ion (negative mode) were authorized as possible primary and seed ions. Replicate samples were
721 grouped and only the features found in 80% of the samples of one group were extracted from the
722 raw data. The obtained lists of features from positive and negative ion modes were merged. The
723 parameters used for metabolite annotation were as follows. The maximum allowed variation on
724 the mass ($\Delta m/z$) was set to 3 ppm, and the maximum mSigma value (assessing the good fitting
725 of isotopic patterns) was set to 30. The merged list of features was annotated using
726 SmartFormula to generate a raw formula based on the exact mass of the primary ions and the
727 isotopic pattern. Analyte lists were derived from KNApSAcK
728 (http://www.knapsackfamily.com/KNApSAcK_Family/), PlantCyc (<https://plantcyc.org/>),

729 FooDB (<http://foodb.ca>), LipidMaps (<https://www.lipidmaps.org/>), and SwissLipids
730 (<https://www.swisslipids.org/>) to obtain a level 3 annotation according to Schymanski
731 classification (tentative candidates based on exact mass and isotopic profile) (Schymanski *et al.*,
732 2014). Spectral libraries (Bruker MetaboBASE Personal Library 3.0,
733 MoNA_LCMSMS_spectra, MSDIAL_LipidBDs-VS34) were searched to obtain level 2
734 annotations (probable structure based on library spectrum match (MS2 data) according to
735 Schymanski *et al.* (2014). PubChem IDs, SMILES and InChiKeys were obtained from PubChem
736 (<https://pubchem.ncbi.nlm.nih.gov/identifiers/>) for chemical enrichment studies
737 using ChemRICH tool (Barupal & Fiehn, 2017).

738 **Sugar determination**

739 Soluble sugar contents were assessed by HPLC (Dionex) according to Rosnoblet *et al.* 2007.
740 Analysis was performed on four replicates of 15 mg of mature Arabidopsis seeds. In brief, Seed
741 were ground in a mortar in the presence of 1 ml 80% methanol containing melizitose as the
742 internal sugar standard. After heating at 76°C for 15 min, the liquid was evaporated under
743 vacuum. The residue was dissolved in 1 ml distilled water and centrifuged for 1 min at 13 000 g.
744 Sugars were analyzed by HPLC on a CarboPac PA-1 column (Dionex Corp.) (Rosnoblet *et al.*,
745 2007).

746 **Targeted hormone analysis**

747 Auxin, ABA and GA were analyzed by ultra-high-performance liquid chromatography (UHPLC)
748 on an UltiMate 3000 UHPLC system (ThermoFisher Scientific) coupled to EvoQ Elite (Bruker)
749 mass spectrometer equipped with an electrospray ionization (ESI) source in MS/MS mode as
750 described in (Zumsteg *et al.*, 2023).

751 **Statistical analyses**

752 Statistical tests were done using a Student-Newman-Keuls test or a two-tailed t-test, implemented
753 in Microsoft Office Excel.

754

755 **Accession Numbers**

756 Sequence data from this article can be found in the GenBank/EMBL data libraries under
757 accession numbers listed in Supplementary Tables 1 and 2.

758

759 **Supplementary Data**

760 Supplementary Figure S1. Untargeted metabolite analysis of mature seeds of *brm3*, *dog1-4* and
761 *brm3 dog1-4*.

762 Supplementary Figure S2. Heatmap showing significant and differential transcript levels of genes
763 of selected pathways.

764 Supplementary Figure S3. HPLC quantification of hormones in dry mature seeds of mutants
765 compared to Col-0 WT.

766 Supplementary Figure S4. UHPLC quantification of total soluble sugars in dry mature seeds of
767 mutants compared to Col-0 WT.

768 Supplementary Figure S5. Glutathione biosynthesis pathway regulation by BRM is *DOG1* gene-
769 dependent.

770 Supplementary Figure S5. Seed physiology is affected in *brm3* mutants compared to wild type.

771 Supplementary Figure S6. Secondary seed dormancy phenotype of the selected mutants.

772 Supplementary Figure S7. Inactivation of SWP73A - BAS SWI/SNF specific subunit - results in
773 stronger dormancy, higher *DOG1* expression and decreased expression of *asDOG1*.

774 Supplementary Figure S8. ChIP-qPCR on BRM binding to *DOG1* locus.

775 Supplementary Figure S10. RT-qPCR expression analysis of the *DOG1* mRNA level.

776 Supplementary Figure S11. RT-qPCR analysis of selected ABA and GA marker genes during
777 secondary dormancy induction.

778 Supplementary Figure S12. RT-qPCR analysis of selected ABA and GA marker genes in *dog1-4*
779 mutant.

780 Supplementary Figure S13. RT-qPCR expression analysis of the native *DOG1* vs *LUC::DOG1*
781 transgene with *dTATA* mutations in antisense region of independent transgenic lines.

782 Supplementary Figure S14. Primary seed dormancy phenotype of *3xbrd*, *brm-3*, *dog1-4* and
783 double *brm-3dog1-4* mutants in comparison to Col-0 WT seeds.

784 Supplementary Figure S15. *DOG1* gene scheme and splicing analysis.

785 Supplementary Table S1. GO terms and ChemRICH metabolite analyses.

786 Supplementary Table S2. List of all primers used in this study.

787 **Funding**

788 This work was funded by a National Science Centre, Poland OPUS16 grant (UMO-
789 2018/31/B/NZ3/03363), SONATA BIS UMO-2018/30/E/NZ1/00354. SPS was supported by a
790 NCN Preludium grant UMO-2015/17/N/NZ2/01919. JZ funded by European Union's Horizon
791 H2020 research and innovation programme under the Marie Skłodowska-Curie grant agreement
792 No 101038075 and from EMBO scientific exchange grant No 9107.

793

794 **Acknowledgments**

795 The authors thank Dimitri Heintz (metabolomics platform) and Jérôme Mutterer (Imaging
796 platform) from IBMP institute, for their help and support. The authors declare that they have no
797 conflict of interest.

798 **Author Contributions**

799 RY and SS conceived and designed the research project. RY, MW, JZ, MK, SPS, RA, CV, JZ,
800 BC, PM and MN performed experiments. RY, MK, JZ, CV, JZ, HS, JB and SS analyzed data.
801 RY and SS wrote the paper with contribution of all authors.

802 **Data availability**

803 The 3'RNA-seq data generated for this study have been deposited at the Gene Expression
804 Omnibus (GEO) under the accession code GSE251921.

805

806

807 **Figure Legends**

808 **Figure 1. Seeds transcriptome and metabolome of *brm* and *dog1* single and double mutants.**
809 **A.** Identification of differentially expressed genes in mature, dry *brm-3*, *dog1-4* and *brm-3dog1-*
810 *4* seeds compared to Col-0 Wild Type (3'RNA-seq, differential analysis was performed using
811 DESeq2 – genes with FDR < 0.05 and absolute fold change > 1 were considered as differentially
812 expressed). **B.** Analysis of overlap between genes whose expression was affected in analyzed
813 mutants (extended graph version shown in Supplementary Figure S1C). **C.** Self-clustering of
814 expression profiles for genes differentially expressed in *brm-3*, identifies the *DOG1*-dependent
815 genes among ones affected in *brm* mutant seeds. Number of DEGs is indicated on panels. **D.**
816 Heatmap of genes' expression for genes misregulated in *brm-3* mutant across mutants used.

817 Genes marked as *DOG1*-gene dependent show suppression of the *brm* effect in the double *brm*-
 818 *3dog1-4* mutant. Second column colors correspond to specific color of the cluster. **E.** Chemical
 819 enrichment analysis of *brm* and *dog* single and double mutants. Colored circles represent clusters
 820 of metabolites from given chemical families (red, increased cluster; blue, decreased cluster;
 821 purple, increased and decreased metabolites in a cluster). The number of metabolites as indicated
 822 as circle size. **F.** The graph represents the fold change of glutathione levels compared to Col-0 in
 823 the seeds of mutants indicated values were ranked into groups as indicated by the respective
 824 letter using a Student-Newman-Keuls test, n=?.

825
 826 **Figure 2. The *brm-3* mutant seeds showed multiple morphological and physiological defects.**
 827 **A.** Scanning electron visualisation of seed from Col-0 WT, *brm-3*, *dog1-4* and *brm-3dog1-4*
 828 mutants. Bar corresponds to 200 nm. **B.** Seeds size analysed using Boxed robot, **C.** Seed yield
 829 analysed based on total number of seeds produced by mature plants. **D.** Seed longevity analysed
 830 using artificial aging. **E.** Germination in presence and absence of 100mM NaCl. **F.** Primary seed
 831 dormancy analysed with freshly harvested seeds. **G.** Secondary dormancy analysis for seed of
 832 *brm-3*, *dog1-4* and *brm-3dog1-4* mutants. Asterisks indicate significant differences compared to
 833 Col-0 dry seeds. Statistical analysis applies to all figure panels; t-test, *, P<0.05, **, P<0.01 and
 834 ***, P<0.0001; n=4, one biological replicate is a mixture of independent 5 plants; error bars
 835 represent standard deviation.

836
 837 **Figure 3. BRM directly regulates *DOG1* antisense transcription to control seed secondary**
 838 **dormancy.** **A.** BRM ChIP-qPCR in dry seeds and **B.** seeds subjected to 3 days of secondary
 839 dormancy induction. Col-0 and BRM-GFP *brm-1* seeds were analysed using GFP antibodies. x-
 840 axis shows beginning of amplicon relative to TSS, TSS=0. Percent of input normalized to PP2A
 841 gene region. **C.** RT-qPCR analysis of *DOG1* sense and **D.** antisense transcripts in Col-0, *brm-3*
 842 and *3xbrd* mutants during secondary dormancy induction; **E.** RT-qPCR analysis of reporter lines
 843 activity during secondary dormancy induction for *p_{sense}DOG1-LUC* and **F.** *p_{AS}DOG1-LUC* lines
 844 in Col-0 and *brm-3* background. **G.** RT-qPCR for endogenous and *LUC-DOG1 deltaTATA* line
 845 activity during secondary dormancy induction shows that inactivation of *asDOG1* results in
 846 stronger induction of *DOG1* during secondary dormancy induction. **H.** BRM, SWP73A and
 847 BRD1 genes expression analysis during SD induction in Arabidopsis seeds. RT-qPCR analysis
 848 in C-H is normalized using *UBC21* gene. Statistical analysis applies to all figure panels, t-test, *,
 849 P<0.05, **, P<0.01 and ***, P<0.0001; n=4, one biological replicate is a mixture of independent
 850 5 plants; error bars represent standard deviation.

851

852 Figure 4. **The *brm3* mutant shows enhanced chromatin accessibility at *DOG1* 3'end during**
853 **secondary dormancy induction.** A. FAIRE in Col-0 and *brm-3* seeds on the 3rd day and B. 5th
854 day of secondary dormancy induction. Chromatin accessibility at *DOG1* shown as % recovery to
855 non-crosslinked samples (UNFAIRE) and relative to PP2A. The x-axis shows beginning of
856 amplicon relative to TSS, TSS=0. C-F. RT-qPCR analysis of α -, β -, γ -, δ -*DOG1* mRNA splicing
857 forms during secondary seed dormancy induction. Transcript level of short (G) and long (H)
858 polyadenylated *DOG1* mRNA forms The x-axis shows time/days of secondary dormancy
859 induction. Statistical analysis applies to all figure panels; t-test, *, P<0.05, **, P<0.01 and ***,
860 P<0.0001; n=4, one biological replicate is a mixture of independent 5 plants; error bars represent
861 standard deviation.

862

863 Figure 5. **Model of the BRAHMA-associated SWI/SNF complex control of Arabidopsis**
864 **seeds quality and physiology.** The BRAHMA-associated SWI/SNF complex controls seed
865 yield, seed size and plant hormonal crosstalk to a large extent independently of *DOG1*. The
866 BRAHMA controls longevity and secondary dormancy by controlling *DOG1* expression through
867 *DOG1* antisense (in red color; dark grey arrows). The BRAHMA also either directly or through
868 *DOG1* antisense negatively controls *DOG1* gene expression (grey arrow) by affecting its
869 alternative splicing and alternative polyadenylation.

870

871 **References**

- 872 **Archacki R, Yatusевич R, Buszewicz D, Krzyczmonik K, Patryn J, Iwanicka-Nowicka R,**
873 **Biecek P, Wilczynski B, Koblowska M, Jerzmanowski A, et al. 2016.** Arabidopsis SWI/SNF
874 chromatin remodeling complex binds both promoters and terminators to regulate gene
875 expression. *Nucleic Acids Research*: gkw1273.
- 876 **Barupal DK, Fiehn O. 2017.** Chemical Similarity Enrichment Analysis (ChemRICH) as
877 alternative to biochemical pathway mapping for metabolomic datasets. *Scientific Reports* 7:
878 14567.
- 879 **Baskin CC, Baskin JM. 2014.** Variation in Seed Dormancy and Germination within and
880 between Individuals and Populations of a Species. In: *Seeds*. Elsevier, 277–373.
- 881 **Bentsink L, Alonso-Blanco C, Vreugdenhil D, Tesnier K, Groot SPC, Koornneef M. 2000.**
882 Genetic Analysis of Seed-Soluble Oligosaccharides in Relation to Seed Storability of
883 Arabidopsis. *Plant Physiology* 124: 1595–1604.
- 884 **Bentsink L, Jowett J, Hanhart CJ, Koornneef M. 2006.** Cloning of DOG1, a quantitative trait
885 locus controlling seed dormancy in Arabidopsis. *Proceedings of the National Academy of*
886 *Sciences of the United States of America* 103: 17042–17047.
- 887 **Bieluszewski T, Prakash S, Roulé T, Wagner D. 2023.** The Role and Activity of SWI/SNF
888 Chromatin Remodelers. *Annual Review of Plant Biology* 74: 139–163.
- 889 **Brzezinka K, Altmann S, Czesnick H, Nicolas P, Gorka M, Benke E, Kabelitz T, Jähne F,**
890 **Graf A, Kappel C, et al. 2016.** Arabidopsis FORGETTER1 mediates stress-induced chromatin
891 memory through nucleosome remodeling. *eLife* 5: e17061.
- 892 **Buijs G. 2020.** A Perspective on Secondary Seed Dormancy in Arabidopsis thaliana. *Plants* 9:
893 749.
- 894 **Cadman CSC, Toorop PE, Hilhorst HWM, Finch-Savage WE. 2006.** Gene expression
895 profiles of Arabidopsis Cvi seeds during dormancy cycling indicate a common underlying
896 dormancy control mechanism. *The Plant Journal* 46: 805–822.
- 897 **Cairns NG, Pasternak M, Wachter A, Cobbett CS, Meyer AJ. 2006.** Maturation of
898 Arabidopsis Seeds Is Dependent on Glutathione Biosynthesis within the Embryo. *Plant*
899 *Physiology* 141: 446–455.
- 900 **Carrillo-Barral N, Rodríguez-Gacio M del C, Matilla AJ. 2020.** Delay of Germination-1
901 (DOG1): A Key to Understanding Seed Dormancy. *Plants* 9: 480.
- 902 **Chang G, Wang C, Kong X, Chen Q, Yang Y, Hu X. 2018.** AFP2 as the novel regulator
903 breaks high-temperature-induced seeds secondary dormancy through ABI5 and SOM in
904 Arabidopsis thaliana. *Biochemical and Biophysical Research Communications* 501: 232–238.
- 905 **Cyrek M, Fedak H, Ciesielski A, Guo Y, Sliwa A, Brzezniak L, Krzyczmonik K, Pietras Z,**
906 **Kaczanowski S, Liu F, et al. 2016.** Seed Dormancy in Arabidopsis Is Controlled by Alternative
907 Polyadenylation of *DOG1*. *Plant Physiology* 170: 947–955.

- 908 **De Souza Vidigal D, Willems L, Van Arkel J, Dekkers BJW, Hilhorst HWM, Bentsink L.**
909 **2016.** Galactinol as marker for seed longevity. *Plant Science* 246: 112–118.
- 910 **Dekkers BJW, Pearce SP, van Bolderen-Veldkamp RPM, Holdsworth MJ, Bentsink L.**
911 **2016.** Dormant and after-ripened *Arabidopsis thaliana* seeds are distinguished by early
912 transcriptional differences in the imbibed state. *Frontiers in Plant Science* 7: 1323.
- 913 **Dekkers BJW, Pearce S, van Bolderen-Veldkamp RP, Marshall A, Widera P, Gilbert J,**
914 **Drost H-G, Bassel GW, Müller K, King JR, et al. 2013.** Transcriptional Dynamics of Two
915 Seed Compartments with Opposing Roles in *Arabidopsis* Seed Germination. *Plant Physiology*
916 163: 205–215.
- 917 **Ding X, Jia X, Xiang Y, Jiang W. 2022.** Histone Modification and Chromatin Remodeling
918 During the Seed Life Cycle. *Frontiers in Plant Science* 13: 865361.
- 919 **Dolata J, Guo Y, Kołowerzo A, Smoliński D, Brzyżek G, Jarmolowski A, Świeżewski S.**
920 **2015.** NTR 1 is required for transcription elongation checkpoints at alternative exons in
921 *Arabidopsis*. *The EMBO Journal* 34: 544–558.
- 922 **Farrona S, Hurtado L, Bowman JL, Reyes JC. 2004.** The *Arabidopsis thaliana* SNF2
923 homolog AtBRM controls shoot development and flowering. *Development* 131: 4965–4975.
- 924 **Farrona S, Hurtado L, Reyes JC. 2007.** A Nucleosome Interaction Module Is Required for
925 Normal Function of *Arabidopsis thaliana* BRAHMA. *Journal of Molecular Biology* 373: 240–
926 250.
- 927 **Fedak H, Palusinska M, Krzyczmonik K, Brzezniak L, Yatusevich R, Pietras Z,**
928 **Kaczanowski S, Swiezewski S. 2016.** Control of seed dormancy in *Arabidopsis* by a *cis*-acting
929 noncoding antisense transcript. *Proceedings of the National Academy of Sciences* 113: E7846–
930 E7855.
- 931 **Finch-Savage WE, Leubner-Metzger G. 2006.** Seed dormancy and the control of germination.
932 *New Phytologist* 171: 501–523.
- 933 **Footitt S, Müller K, Kermodé AR, Finch-Savage WE. 2015.** Seed dormancy cycling in A
934 *rabidopsis*: chromatin remodelling and regulation of DOG 1 in response to seasonal
935 environmental signals. *The Plant Journal* 81: 413–425.
- 936 **Footitt S, Ölçer-Footitt H, Hambidge AJ, Finch-Savage WE. 2017.** A laboratory simulation
937 of *Arabidopsis* seed dormancy cycling provides new insight into its regulation by clock genes
938 and the dormancy-related genes *DOG1*, *MFT*, *CIPK23* and *PHYA*: Dormancy cycling with
939 mutants. *Plant, Cell & Environment* 40: 1474–1486.
- 940 **Fu W, Yu Y, Shu J, Yu Z, Zhong Y, Zhu T, Zhang Z, Liang Z, Cui Y, Chen C, et al. 2023.**
941 Organization, genomic targeting, and assembly of three distinct SWI/SNF chromatin remodeling
942 complexes in *Arabidopsis*. *The Plant Cell* 35: 2464–2483.
- 943 **Guo J, Cai G, Li Y-Q, Zhang Y-X, Su Y-N, Yuan D-Y, Zhang Z-C, Liu Z-Z, Cai X-W, Guo**
944 **J, et al. 2022a.** Comprehensive characterization of three classes of *Arabidopsis* SWI/SNF
945 chromatin remodelling complexes. *Nature Plants* 8: 1423–1439.

- 946 **Guo P, Hoang N, Sanchez J, Zhang EH, Rajawasam K, Trinidad K, Sun H, Zhang H.**
 947 **2022b.** The assembly of mammalian SWI/SNF chromatin remodeling complexes is regulated by
 948 lysine-methylation dependent proteolysis. *Nature Communications* 13: 6696.
- 949 **Han S-K, Sang Y, Rodrigues A, BIOL425 F2010, Wu M-F, Rodriguez PL, Wagner D. 2012.**
 950 The SWI2/SNF2 Chromatin Remodeling ATPase BRAHMA Represses Abscisic Acid
 951 Responses in the Absence of the Stress Stimulus in Arabidopsis. *The Plant Cell* 24: 4892–4906.
- 952 **Hauvermale AL, Tuttle KM, Takebayashi Y, Seo M, Steber CM. 2015.** Loss of *Arabidopsis*
 953 *thaliana* Seed Dormancy is Associated with Increased Accumulation of the GID1 GA Hormone
 954 Receptors. *Plant and Cell Physiology* 56: 1773–1785.
- 955 **He H, Willems LAJ, Batushansky A, Fait A, Hanson J, Nijveen H, Hilhorst HWM,**
 956 **Bentsink L. 2016.** Effects of Parental Temperature and Nitrate on Seed Performance are
 957 Reflected by Partly Overlapping Genetic and Metabolic Pathways. *Plant and Cell Physiology* 57:
 958 473–487.
- 959 **Hernández-García J, Diego-Martin B, Kuo PH, Jami-Alahmadi Y, Vashisht AA,**
 960 **Wohlschlegel J, Jacobsen SE, Blázquez MA, Gallego-Bartolomé J. 2022.** Comprehensive
 961 identification of SWI/SNF complex subunits underpins deep eukaryotic ancestry and reveals new
 962 plant components. *Communications Biology* 5: 549.
- 963 **Holdsworth MJ, Bentsink L, Soppe WJJ. 2008.** Molecular networks regulating Arabidopsis
 964 seed maturation, after-ripening, dormancy and germination. *New Phytologist* 179: 33–54.
- 965 **Hurtado L, Farrona S, Reyes JC. 2006.** The putative SWI/SNF complex subunit BRAHMA
 966 activates flower homeotic genes in Arabidopsis thaliana. *Plant Molecular Biology* 62: 291–304.
- 967 **Ibarra SE, Tognacca RS, Dave A, Graham IA, Sánchez RA, Botto JF. 2016.** Molecular
 968 mechanisms underlying the entrance in secondary dormancy of *Arabidopsis* seeds: Mechanisms
 969 underlying secondary dormancy. *Plant, Cell & Environment* 39: 213–221.
- 970 **Iwasaki M, Penfield S, Lopez-Molina L. 2022.** Parental and Environmental Control of Seed
 971 Dormancy in *Arabidopsis thaliana*. *Annual Review of Plant Biology* 73: 355–378.
- 972 **Jarończyk K, Sosnowska K, Zaborowski A, Pupel P, Bucholc M, Malecka E, Siwirykow N,**
 973 **Stachula P, Iwanicka-Nowicka R, Kobłowska M, et al. 2021.** Bromodomain-containing
 974 subunits BRD1, BRD2, and BRD13 are required for proper functioning of SWI/SNF complexes
 975 in Arabidopsis. *Plant Communications* 2: 100174.
- 976 **Jégu T, Veluchamy A, Ramirez-Prado JS, Rizzi-Paillet C, Perez M, Lhomme A, Latrasse**
 977 **D, Coleno E, Vicaire S, Legras S, et al. 2017.** The Arabidopsis SWI/SNF protein BAF60
 978 mediates seedling growth control by modulating DNA accessibility. *Genome Biology* 18: 114.
- 979 **Koramutla MK, Negi M, Ayele BT. 2021.** Roles of Glutathione in Mediating Abscisic Acid
 980 Signaling and Its Regulation of Seed Dormancy and Drought Tolerance. *Genes* 12: 1620.
- 981 **Krzyszton M, Sacharowski SP, Sanchez F, Muter K, Dobisova T, Swiezewski S. 2022.**
 982 Single seeds exhibit transcriptional heterogeneity during secondary dormancy induction. *Plant*
 983 *Physiology* 190: 211–225.

- 984 **Kumar S, Kaur A, Chattopadhyay B, Bachhawat AK. 2015.** Defining the cytosolic pathway
985 of glutathione degradation in *Arabidopsis thaliana* : role of the ChaC/GCG family of γ -glutamyl
986 cyclotransferases as glutathione-degrading enzymes and AtLAP1 as the Cys-Gly peptidase.
987 *Biochemical Journal* 468: 73–85.
- 988 **Lefebvre V, North H, Frey A, Sotta B, Seo M, Okamoto M, Nambara E, Marion-Poll A.**
989 **2006.** Functional analysis of *Arabidopsis NCED6* and *NCED9* genes indicates that ABA
990 synthesized in the endosperm is involved in the induction of seed dormancy. *The Plant Journal*
991 45: 309–319.
- 992 **Li T, Zhang Y, Wang D, Liu Y, Dirk LMA, Goodman J, Downie AB, Wang J, Wang G,**
993 **Zhao T. 2017.** Regulation of Seed Vigor by Manipulation of Raffinose Family Oligosaccharides
994 in Maize and *Arabidopsis thaliana*. *Molecular Plant* 10: 1540–1555.
- 995 **Mashtalir N, D’Avino AR, Michel BC, Luo J, Pan J, Otto JE, Zullo HJ, McKenzie ZM,**
996 **Kubiak RL, St. Pierre R, et al. 2018.** Modular Organization and Assembly of SWI/SNF Family
997 Chromatin Remodeling Complexes. *Cell* 175: 1272-1288.e20.
- 998 **Mhamdi A, Hager J, Chaouch S, Queval G, Han Y, Taconnat L, Saindrenan P, Gouia H,**
999 **Issakidis-Bourguet E, Renou J-P, et al. 2010.** *Arabidopsis* GLUTATHIONE REDUCTASE1
1000 Plays a Crucial Role in Leaf Responses to Intracellular Hydrogen Peroxide and in Ensuring
1001 Appropriate Gene Expression through Both Salicylic Acid and Jasmonic Acid Signaling
1002 Pathways. *Plant Physiology* 153: 1144–1160.
- 1003 **Montez M, Majchrowska M, Krzyszton M, Bokota G, Sacharowski S, Wrona M,**
1004 **Yatusevich R, Massana F, Plewczynski D, Swiezewski S. 2023.** Promoter-pervasive
1005 transcription causes RNA polymerase II pausing to boost *DOG1* expression in response to salt.
1006 *The EMBO journal* 42: e112443.
- 1007 **Nguyen T-P, Cueff G, Hegedus DD, Rajjou L, Bentsink L. 2015.** A role for seed storage
1008 proteins in *Arabidopsis* seed longevity. *Journal of Experimental Botany* 66: 6399–6413.
- 1009 **Nguyen T-P, Keizer P, Van Eeuwijk F, Smeekens S, Bentsink L. 2012.** Natural Variation for
1010 Seed Longevity and Seed Dormancy Are Negatively Correlated in *Arabidopsis*. *Plant*
1011 *Physiology* 160: 2083–2092.
- 1012 **Nguyen VPT, Stewart J, Lopez M, Ioannou I, Allais F. 2020.** Glucosinolates: Natural
1013 Occurrence, Biosynthesis, Accessibility, Isolation, Structures, and Biological Activities.
1014 *Molecules* 25: 4537.
- 1015 **Ojolo SP, Cao S, Priyadarshani SVGN, Li W, Yan M, Aslam M, Zhao H, Qin Y. 2018.**
1016 Regulation of Plant Growth and Development: A Review From a Chromatin Remodeling
1017 Perspective. *Frontiers in Plant Science* 9: 1232.
- 1018 **Omidbakhshfard MA, Winck FV, Arvidsson S, Riaño-Pachón DM, Mueller-Roeber B.**
1019 **2014.** A step-by-step protocol for formaldehyde-assisted isolation of regulatory elements from
1020 *Arabidopsis thaliana*. *Journal of Integrative Plant Biology* 56: 527–538.
- 1021 **Ranganathan U, Groot SPC. 2023.** Seed Longevity and Deterioration. In: Dadlani M, Yadava
1022 DK, eds. *Seed Science and Technology*. Singapore: Springer Nature Singapore, 91–108.

- 1023 **Rosnoblet C, Aubry C, Leprince O, Vu BL, Rogniaux H, Buitink J. 2007.** The regulatory
1024 gamma subunit SNF4b of the sucrose non-fermenting-related kinase complex is involved in
1025 longevity and stachyose accumulation during maturation of *Medicago truncatula* seeds. *The*
1026 *Plant Journal* 51: 47–59.
- 1027 **Sacharowski SP, Gratkowska DM, Sarnowska EA, Kondrak P, Jancewicz I, Porri A,**
1028 **Bucior E, Rolicka AT, Franzen R, Kowalczyk J, et al. 2015.** SWP73 Subunits of Arabidopsis
1029 SWI/SNF Chromatin Remodeling Complexes Play Distinct Roles in Leaf and Flower
1030 Development. *The Plant Cell* 27: 1889–1906.
- 1031 **Sajeev N, Koornneef M, Bentsink L. 2024.** A commitment for *life*: Decades of unraveling the
1032 molecular mechanisms behind seed dormancy and germination. *The Plant Cell*: koad328.
- 1033 **Salvi P, Varshney V, Majee M. 2022.** Raffinose family oligosaccharides (RFOs): role in seed
1034 vigor and longevity. *Bioscience Reports* 42: BSR20220198.
- 1035 **Sano N, Marion-Poll A. 2021.** ABA Metabolism and Homeostasis in Seed Dormancy and
1036 Germination. *International Journal of Molecular Sciences* 22: 5069.
- 1037 **Sano N, Rajjou L, North HM, Debeaujon I, Marion-Poll A, Seo M. 2016.** Staying Alive:
1038 Molecular Aspects of Seed Longevity. *Plant and Cell Physiology* 57: 660–674.
- 1039 **Schymanski EL, Jeon J, Gulde R, Fenner K, Ruff M, Singer HP, Hollender J. 2014.**
1040 Identifying Small Molecules via High Resolution Mass Spectrometry: Communicating
1041 Confidence. *Environmental Science & Technology* 48: 2097–2098.
- 1042 **Shang J, He X. 2022.** Chromatin-remodeling complexes: Conserved and plant-specific subunits
1043 in *Arabidopsis*. *Journal of Integrative Plant Biology* 64: 499–515.
- 1044 **Skubacz A, Daszkowska-Golec A. 2017.** Seed Dormancy: The Complex Process Regulated by
1045 Abscisic Acid, Gibberellins, and Other Phytohormones that Makes Seed Germination Work. In:
1046 El-Esawi M, ed. *Phytohormones - Signaling Mechanisms and Crosstalk in Plant Development*
1047 *and Stress Responses*. InTech.
- 1048 **Stachula P, Kapela K, Malecka E, Jaronczyk K, Patryn J, Siwirykow N, Bucholc M,**
1049 **Marczak M, Kotlinski M, Archacki R. 2023.** BRM Complex in Arabidopsis Adopts ncBAF-
1050 like Composition and Requires BRD Subunits for Assembly and Stability. *International Journal*
1051 *of Molecular Sciences* 24: 3917.
- 1052 **Stotz HU, Sawada Y, Shimada Y, Hirai MY, Sasaki E, Krischke M, Brown PD, Saito K,**
1053 **Kamiya Y. 2011.** Role of camalexin, indole glucosinolates, and side chain modification of
1054 glucosinolate-derived isothiocyanates in defense of Arabidopsis against *Sclerotinia sclerotiorum*.
1055 *The Plant Journal* 67: 81–93.
- 1056 **Tang X, Hou A, Babu M, Nguyen V, Hurtado L, Lu Q, Reyes JC, Wang A, Keller WA,**
1057 **Harada JJ, et al. 2008.** The Arabidopsis BRAHMA chromatin-remodeling ATPase is involved
1058 in repression of seed maturation genes in leaves. *Plant Physiology* 147: 1143–1157.
- 1059 **Tognacca RS, Botto JF. 2021.** Post-transcriptional regulation of seed dormancy and
1060 germination: Current understanding and future directions. *Plant Communications* 2: 100169.

- 1061 **Yatusevich R, Fedak H, Ciesielski A, Krzyczmonik K, Kulik A, Dobrowolska G,**
1062 **Swiezewski S. 2017.** Antisense transcription represses *Arabidopsis* seed dormancy QTL *DOG 1*
1063 to regulate drought tolerance. *EMBO reports* 18: 2186–2196.
- 1064 **Yu X, Willmann MR, Vandivier LE, Trefely S, Kramer MC, Shapiro J, Guo R, Lyons E,**
1065 **Snyder NW, Gregory BD. 2021.** Messenger RNA 5' NAD⁺ capping is a dynamic regulatory
1066 epitranscriptome mark that is required for proper response to abscisic acid in *Arabidopsis*.
1067 *Developmental Cell* 56: 125-140.e6.
- 1068 **Yu Y, Liang Z, Song X, Fu W, Xu J, Lei Y, Yuan L, Ruan J, Chen C, Fu W, et al (2020)**
1069 **BRAHMA-interacting proteins BRIP1 and BRIP2 are core subunits of Arabidopsis SWI/SNF**
1070 **complexes. Nat Plants 6: 996–1007**
- 1071 **Yu Y, Fu W, Xu J, Lei Y, Song X, Liang Z, Zhu T, Liang Y, Hao Y, Yuan L, et al (2021)**
1072 **Bromodomain-containing proteins BRD1, BRD2, and BRD13 are core subunits of SWI/SNF**
1073 **complexes and vital for their genomic targeting in Arabidopsis. Molecular Plant 14: 888–904**
- 1074 **Zinsmeister J, Leprince O, Buitink J. 2020.** Molecular and environmental factors regulating
1075 seed longevity. *Biochemical Journal* 477: 305–323.
- 1076 **Zumsteg J, Bossard E, Gourguillon L, Villette C, Heintz D. 2023.** Comparison of nocturnal
1077 and diurnal metabolomes of rose flowers and leaves. *Metabolomics* 20: 4.

ACCEPTED MANUSCRIPT

Figure 1

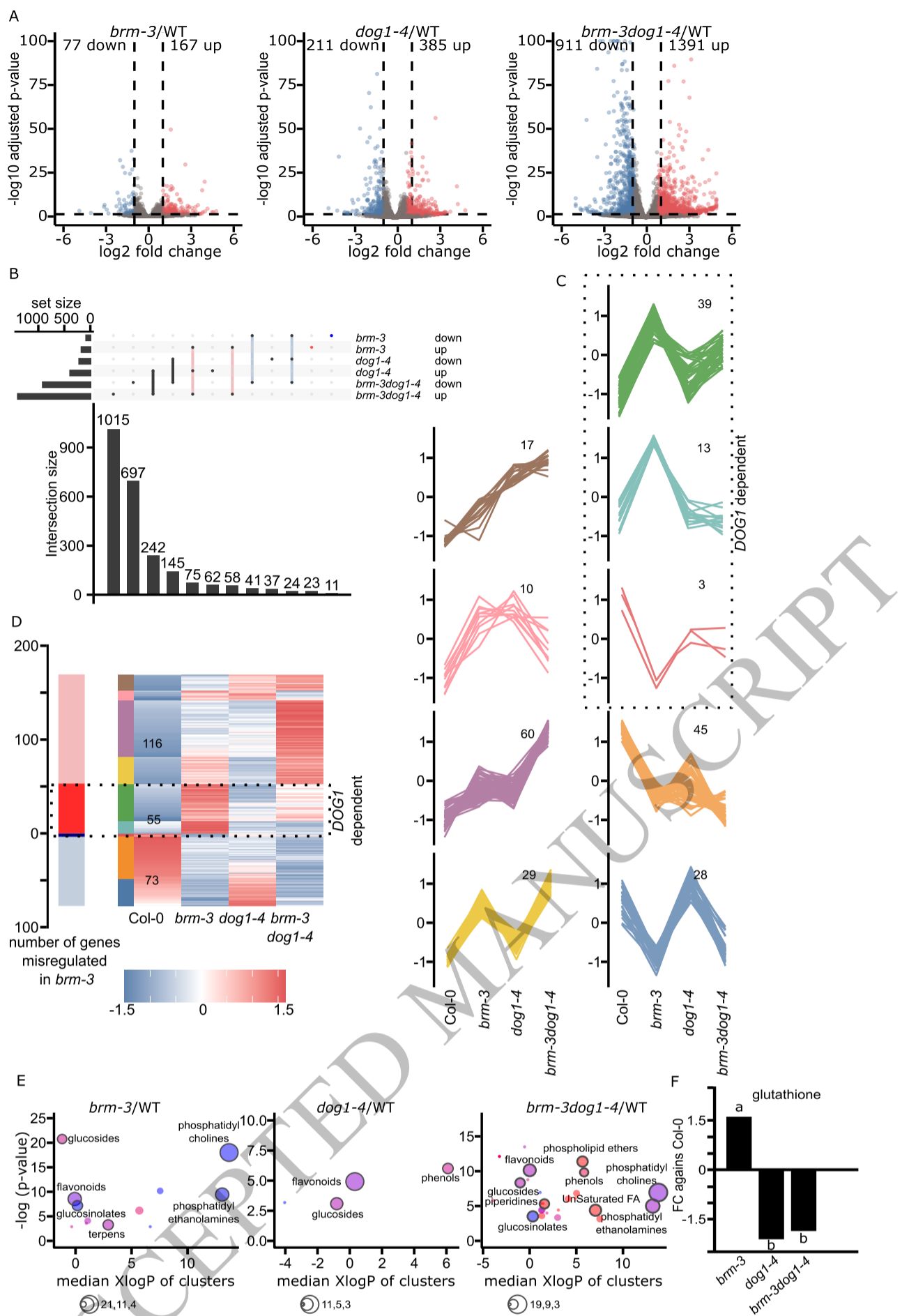


Figure 1. Seeds transcriptome and metabolome of *brm* and *dog1* single and double mutants.

A. Identification of differentially expressed genes in mature, dry *brm-3*, *dog1-4* and *brm-3dog1-4* seeds compared to Col-0 Wild Type (3'RNA-seq, differential analysis was performed DESeq2 – genes with FDR < 0.05 and absolute fold change > 1 were considered as differentially expressed).

B. Analysis of overlap between genes whose expression was affected in analyzed mutants (extended graph version shown in Supplementary Figure S1, the x-axis is set).

C. Self-clustering of expression profiles for genes differentially expressed in *brm-3*, identifies the *DOG1*-dependent genes among ones affected in *brm* mutant seeds. Number of DEGs is indicated on panels. the y-axis is scaled expression.

D. Heatmap of genes' expression for genes misregulated in *brm-3* mutant across mutants used. Genes marked as *DOG1*-gene dependent show suppression of the *brm* effect in the double *brm-3dog1-4* mutant. Second column colors correspond to specific color of the cluster.

E. Chemical enrichment analysis of *brm* and *dog* single and double mutants. Colored circles represent clusters of metabolites from given chemical families (red, increased cluster; blue, decreased cluster; purple, increased and decreased metabolites in a cluster). The number of metabolites as indicated as circle size.

F. The graph represents the fold change of glutathione levels compared to Col-0 in the seeds of mutants indicated values were ranked into groups as indicated by the respective letter using a Student-Newman-Keuls test, n=4.

Figure 2

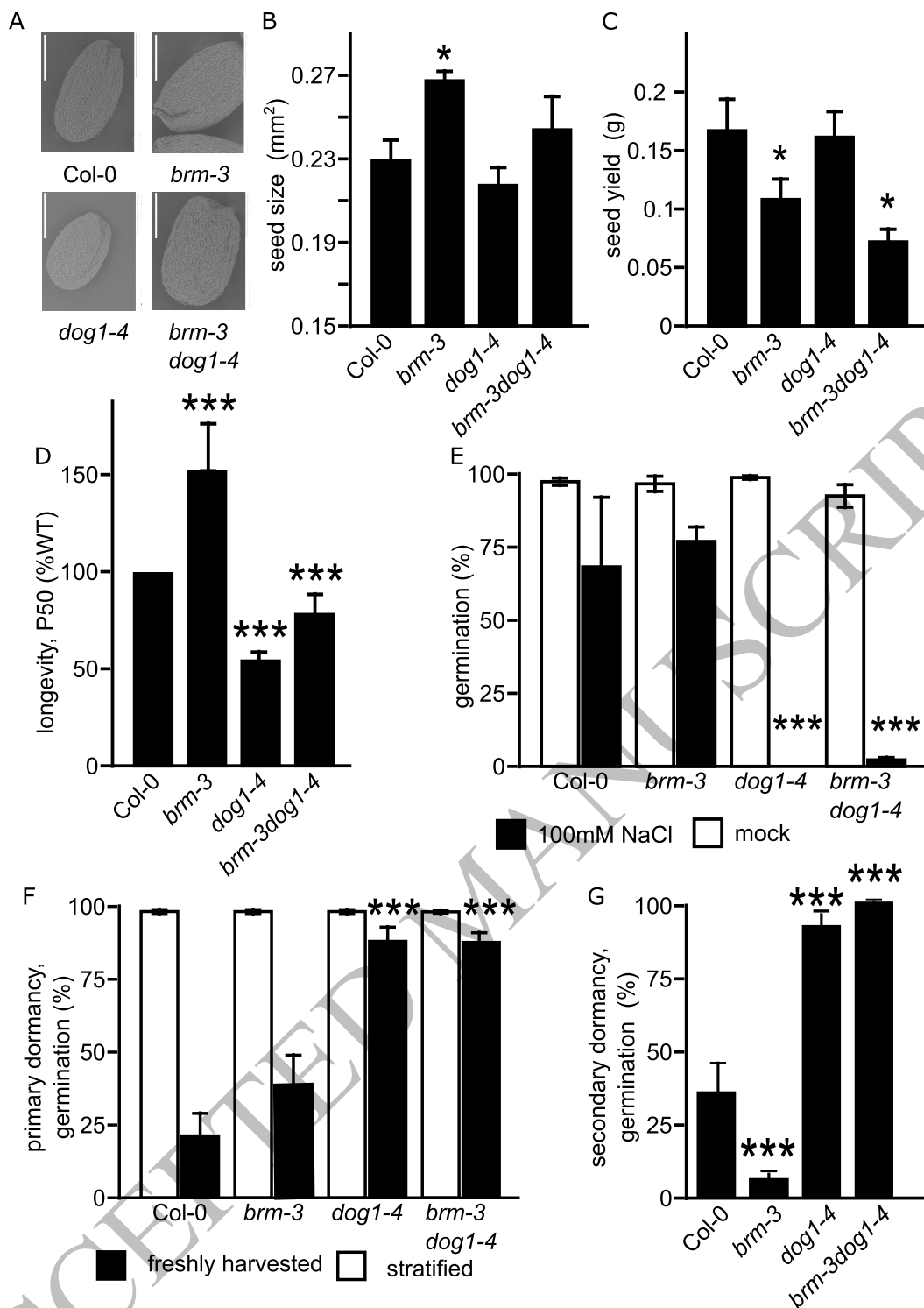


Figure 2. The *brm-3* mutant seeds showed multiple morphological and physiological defects.

A. Scanning electron visualization of seed from Col-0 WT, *brm-3*, *dog1-4* and *brm-3dog1-4* mutants. Bar corresponds to 200 nm. **B.** Seeds size analyzed using Boxed robot, **C.** Seed yield analyzed based on total number of seeds produced by mature plants. **D.** Seed longevity analyzed using artificial aging. **E.** Germination in presence and absence of 100mM NaCl. **F.** Primary seed dormancy analyzed with freshly harvested seeds. **G.** Secondary dormancy analysis for seed of *brm-3*, *dog1-4* and *brm-3dog1-4* mutants. Asterisks indicate significant differences compared to Col-0 dry seeds. Statistical analysis applies to all figure panels; t-test, *, P<0.05, **, P<0.01 and ***, P<0.0001; n=4, one biological replicate is a mixture of independent 5 plants; error bars represent standard deviation (\pm SD).

Figure 3

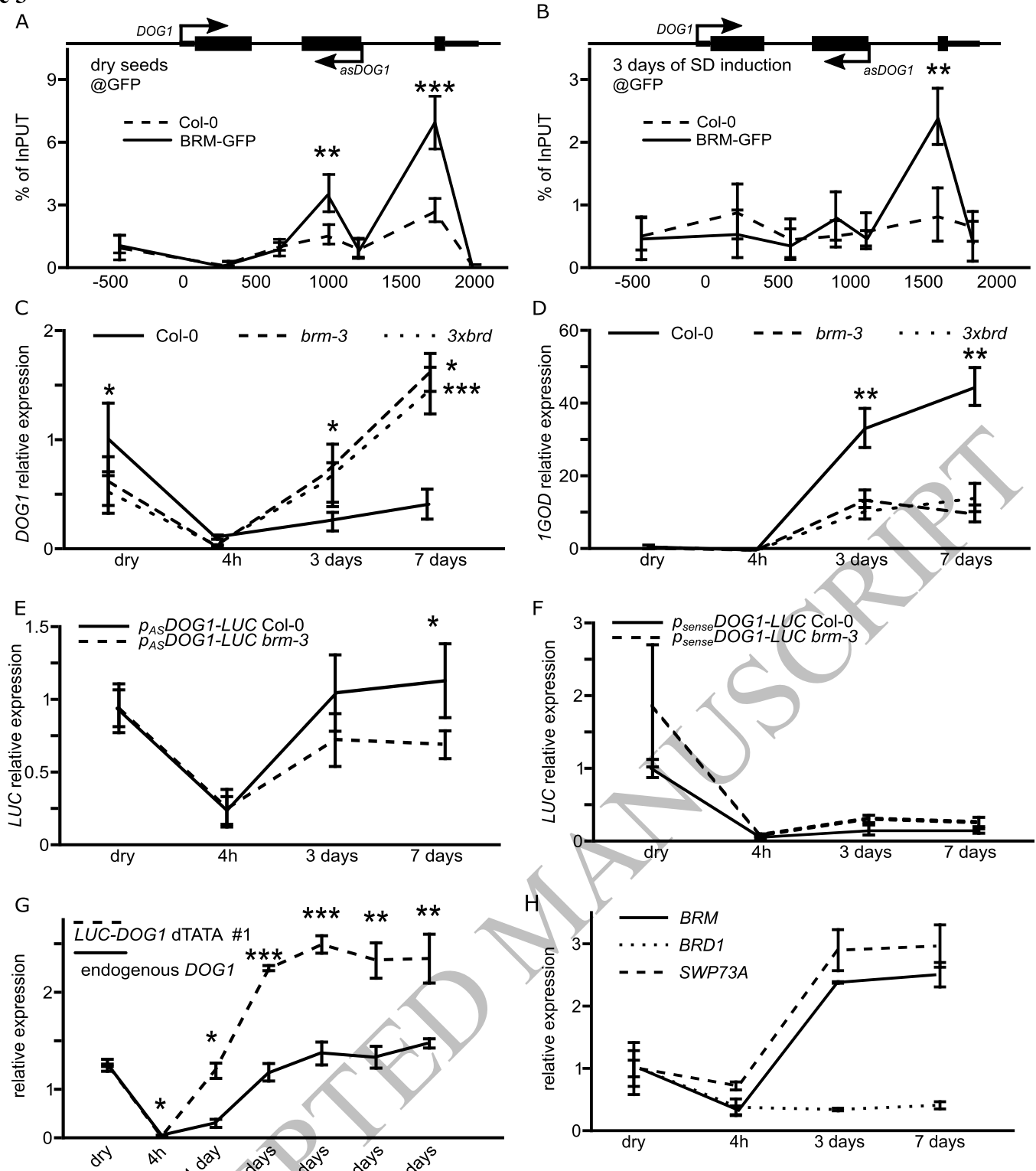


Figure 3. BRM directly regulates *DOG1* antisense transcription to control seed secondary dormancy. **A.** BRM ChIP-qPCR in dry seeds and **B.** seeds subjected to 3 days of secondary dormancy induction. Col-0 and BRM-GFP *brm-1* seeds were analyzed using GFP antibodies. x-axis shows beginning of amplicon relative to TSS, TSS=0. Percent of input normalized to PP2A gene region. **C.** RT-qPCR analysis of *DOG1* sense and **D.** antisense transcripts in Col-0, *brm-3* and *3xbrd* mutants during secondary dormancy induction; **E.** RT-qPCR analysis of reporter lines activity during secondary dormancy induction for *p_{sense}DOG1-LUC* and **F.** *p_{AS}DOG1-LUC* lines in Col-0 and *brm-3* background. **G.** RT-qPCR for endogenous and *LUC-DOG1 deltaTATA* line activity during secondary dormancy induction shows that inactivation of *asDOG1* results in stronger induction of *DOG1* during secondary dormancy induction. **H.** BRM, SWP73A and BRD1 genes expression analysis during SD induction in Arabidopsis seeds. RT-qPCR analysis in C-H is normalized using *UBC21* gene and the x-axis shows time/days of secondary dormancy induction (h-hours; d-days). Statistical analysis applies to all figure panels, t-test, *, P<0.05, **, P<0.01 and ***, P<0.0001; n=4, one biological replicate is a mixture of independent 5 plants; error bars represent standard deviation (\pm SD).

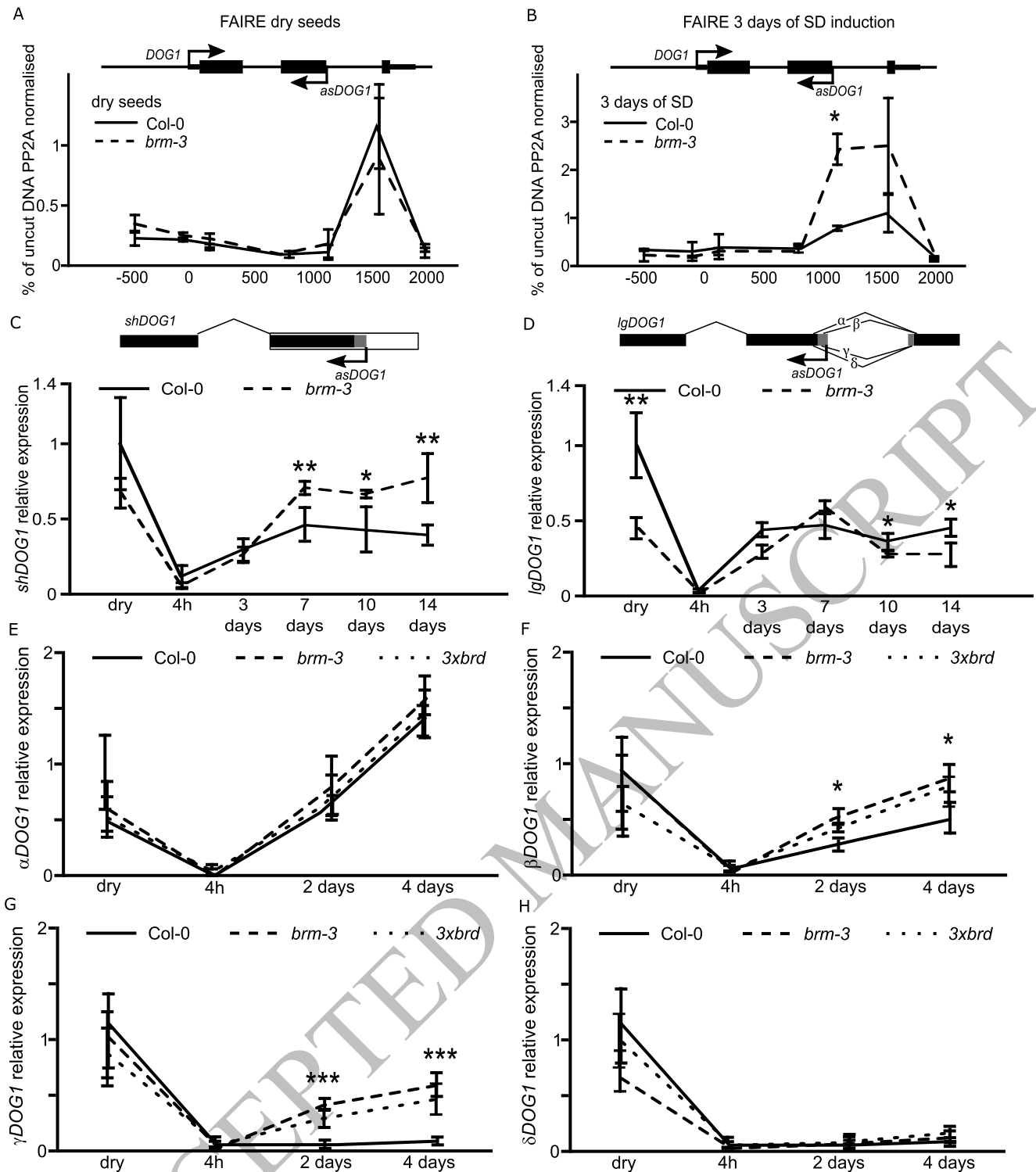
Figure 4

Figure 4. The *brm3* mutant shows enhanced chromatin accessibility at *DOG1* 3'end during secondary dormancy induction. **A.** FAIRE in Col-0 and *brm-3* seeds on the 3rd day and **B.** 5th day of secondary dormancy induction. Chromatin accessibility at *DOG1* shown as % recovery to non-crosslinked samples (UNFAIRE) and relative to PP2A. The x-axis shows beginning of amplicon relative to TSS, TSS=0. **C-F.** RT-qPCR analysis of α -, β -, γ -, δ -*DOG1* mRNA splicing forms during secondary seed dormancy induction. Transcript 1 level of short (**G**) and long (**H**) polyadenylated *DOG1* mRNA forms. The x-axis shows time/days of secondary dormancy induction (h-hours; d-days). Statistical analysis applies to all figure panels; t-test, *, P<0.05, **, P<0.01 and ***, P<0.0001; n=4, one biological replicate is a mixture of independent 5 plants; error bars represent standard deviation (\pm SD).

Figure 5

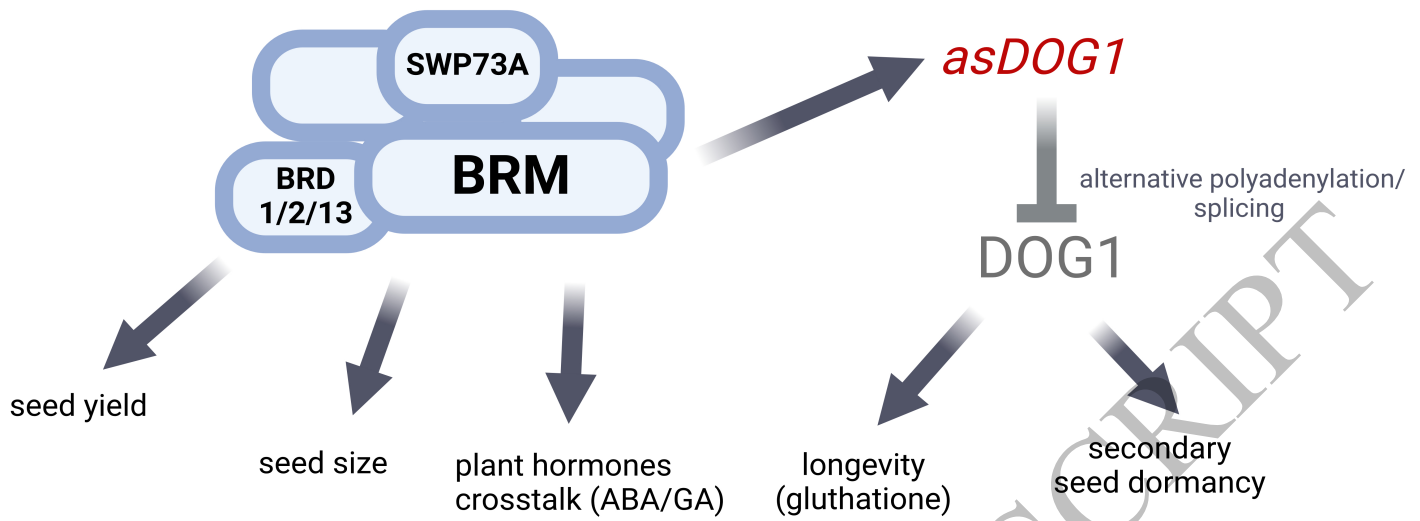


Figure 5. **Model of the BRAHMA-associated SWI/SNF complex control of Arabidopsis seeds quality and physiology.** The BRAHMA-associated SWI/SNF complex controls seed yield, seed size and plant hormonal crosstalk to a large extent independently of DOG1. The BRAHMA controls longevity and secondary dormancy by controlling *DOG1* expression through *DOG1* antisense (in red color; dark grey arrows). The BRAHMA also either directly or through *DOG1* antisense negatively controls *DOG1* gene expression (grey arrow) by affecting its alternative splicing and alternative polyadenylation.

Parsed Citations

- Archacki R, Yatusevich R, Buszewicz D, Krzyczmonik K, Patryn J, Iwanicka-Nowicka R, Biecek P, Wilczynski B, Koblowska M, Jerzmanowski A, et al. 2016. Arabidopsis SW/SNF chromatin remodeling complex binds both promoters and terminators to regulate gene expression. *Nucleic Acids Research*: gkw1273.
Google Scholar: [Author Only](#) [Title Only](#) [Author and Title](#)
- Barupal DK, Fiehn O. 2017. Chemical Similarity Enrichment Analysis (ChemRICH) as alternative to biochemical pathway mapping for metabolomic datasets. *Scientific Reports* 7: 14567.
Google Scholar: [Author Only](#) [Title Only](#) [Author and Title](#)
- Baskin CC, Baskin JM. 2014. Variation in Seed Dormancy and Germination within and between Individuals and Populations of a Species. In: *Seeds*. Elsevier, 277–373.
Google Scholar: [Author Only](#) [Title Only](#) [Author and Title](#)
- Bentsink L, Alonso-Blanco C, Vreugdenhil D, Tesnier K, Groot SPC, Koornneef M. 2000. Genetic Analysis of Seed-Soluble Oligosaccharides in Relation to Seed Storability of Arabidopsis. *Plant Physiology* 124: 1595–1604.
Google Scholar: [Author Only](#) [Title Only](#) [Author and Title](#)
- Bentsink L, Jowett J, Hanhart CJ, Koornneef M. 2006. Cloning of DOG1, a quantitative trait locus controlling seed dormancy in Arabidopsis. *Proceedings of the National Academy of Sciences of the United States of America* 103: 17042–17047.
Google Scholar: [Author Only](#) [Author and Title](#)
- Bieluszewski T, Prakash S, Roulé T, Wagner D. 2023. The Role and Activity of SW/SNF Chromatin Remodelers. *Annual Review of Plant Biology* 74: 139–163.
Google Scholar: [Author Only](#) [Title Only](#) [Author and Title](#)
- Brzezinka K, Altmann S, Czesnick H, Nicolas P, Gorka M, Benke E, Kabelitz T, Jähne F, Graf A, Kappel C, et al. 2016. Arabidopsis FORGETTER1 mediates stress-induced chromatin memory through nucleosome remodeling. *eLife* 5: e17061.
Google Scholar: [Author Only](#) [Title Only](#) [Author and Title](#)
- Buijs G. 2020. A Perspective on Secondary Seed Dormancy in Arabidopsis thaliana. *Plants* 9: 749.
Google Scholar: [Author Only](#) [Title Only](#) [Author and Title](#)
- Cadman CSC, Toorop PE, Hilhorst HWM, Finch-Savage WE. 2006. Gene expression profiles of Arabidopsis Cvi seeds during dormancy cycling indicate a common underlying dormancy control mechanism. *The Plant Journal* 46: 805–822.
Google Scholar: [Author Only](#) [Title Only](#) [Author and Title](#)
- Cairns NG, Pasternak M, Wachter A, Cobbett CS, Meyer AJ. 2006. Maturation of Arabidopsis Seeds Is Dependent on Glutathione Biosynthesis within the Embryo. *Plant Physiology* 141: 446–455.
Google Scholar: [Author Only](#) [Title Only](#) [Author and Title](#)
- Carrillo-Barral N, Rodríguez-Gacio M del C, Matilla AJ. 2020. Delay of Germination-1 (DOG1): A Key to Understanding Seed Dormancy. *Plants* 9: 480.
Google Scholar: [Author Only](#) [Title Only](#) [Author and Title](#)
- Chang G, Wang C, Kong X, Chen Q, Yang Y, Hu X. 2018. AFP2 as the novel regulator breaks high-temperature-induced seeds secondary dormancy through ABI5 and SOM in Arabidopsis thaliana. *Biochemical and Biophysical Research Communications* 501: 232–238.
Google Scholar: [Author Only](#) [Title Only](#) [Author and Title](#)
- Cyrek M, Fedak H, Ciesielski A, Guo Y, Sliwa A, Brzezniak L, Krzyczmonik K, Pietras Z, Kaczanowski S, Liu F, et al. 2016. Seed Dormancy in Arabidopsis Is Controlled by Alternative Polyadenylation of DOG1. *Plant Physiology* 170: 947–955.
Google Scholar: [Author Only](#) [Title Only](#) [Author and Title](#)
- De Souza Vidigal D, Willems L, Van Arkel J, Dekkers BJW, Hilhorst HWM, Bentsink L. 2016. Galactinol as marker for seed longevity. *Plant Science* 246: 112–118.
Google Scholar: [Author Only](#) [Title Only](#) [Author and Title](#)
- Dekkers BJW, Pearce SP, van Bolderen-Veldkamp RPM, Holdsworth MJ, Bentsink L. 2016. Dormant and after-ripened Arabidopsis thaliana seeds are distinguished by early transcriptional differences in the imbibed state. *Frontiers in Plant Science* 7: 1323.
Google Scholar: [Author Only](#) [Title Only](#) [Author and Title](#)
- Dekkers BJW, Pearce S, van Bolderen-Veldkamp RP, Marshall A, Widera P, Gilbert J, Drost H-G, Bassel GW, Müller K, King JR, et al. 2013. Transcriptional Dynamics of Two Seed Compartments with Opposing Roles in Arabidopsis Seed Germination. *Plant Physiology* 163: 205–215.
Google Scholar: [Author Only](#) [Title Only](#) [Author and Title](#)
- Ding X, Jia X, Xiang Y, Jiang W. 2022. Histone Modification and Chromatin Remodeling During the Seed Life Cycle. *Frontiers in*

Plant Science 13: 865361.

Google Scholar: [Author Only](#) [Title Only](#) [Author and Title](#)

Dolata J, Guo Y, Kołowerzo A, Smoliński D, Brzyżek G, Jarmołowski A, Świeżewski S. 2015. NTR 1 is required for transcription elongation checkpoints at alternative exons in Arabidopsis. The EMBO Journal 34: 544–558.

Google Scholar: [Author Only](#) [Title Only](#) [Author and Title](#)

Farrona S, Hurtado L, Bowman JL, Reyes JC. 2004. The Arabidopsis thaliana SNF2 homolog AtBRM controls shoot development and flowering. Development 131: 4965–4975.

Google Scholar: [Author Only](#) [Title Only](#) [Author and Title](#)

Farrona S, Hurtado L, Reyes JC. 2007. A Nucleosome Interaction Module Is Required for Normal Function of Arabidopsis thaliana BRAHMA. Journal of Molecular Biology 373: 240–250.

Google Scholar: [Author Only](#) [Title Only](#) [Author and Title](#)

Fedak H, Palusinska M, Krzyczmonik K, Brzezniak L, Yatusovich R, Pietras Z, Kaczanowski S, Swiezewski S. 2016. Control of seed dormancy in Arabidopsis by a cis -acting noncoding antisense transcript. Proceedings of the National Academy of Sciences 113: E7846–E7855.

Google Scholar: [Author Only](#) [Title Only](#) [Author and Title](#)

Finch-Savage WE, Leubner-Metzger G. 2006. Seed dormancy and the control of germination. New Phytologist 171: 501–523.

Google Scholar: [Author Only](#) [Title Only](#) [Author and Title](#)

Footitt S, Müller K, Kermode AR, Finch-Savage WE. 2015. Seed dormancy cycling in Arabidopsis: chromatin remodelling and regulation of DOG 1 in response to seasonal environmental signals. The Plant Journal 81: 413–425.

Google Scholar: [Author Only](#) [Title Only](#) [Author and Title](#)

Footitt S, Ölçer-Footitt H, Hambidge AJ, Finch-Savage WE. 2017. A laboratory simulation of Arabidopsis seed dormancy cycling provides new insight into its regulation by clock genes and the dormancy-related genes DOG1, MFT, CIPK23 and PHYA: Dormancy cycling with mutants. Plant, Cell & Environment 40: 1474–1486.

Google Scholar: [Author Only](#) [Author and Title](#)

Fu W, Yu Y, Shu J, Yu Z, Zhong Y, Zhu T, Zhang Z, Liang Z, Cui Y, Chen C, et al. 2023. Organization, genomic targeting, and assembly of three distinct SW/SNF chromatin remodeling complexes in Arabidopsis. The Plant Cell 35: 2464–2483.

Google Scholar: [Author Only](#) [Title Only](#) [Author and Title](#)

Guo J, Cai G, Li Y-Q, Zhang Y-X, Su Y-N, Yuan D-Y, Zhang Z-C, Liu Z-Z, Cai X-W, Guo J, et al. 2022a. Comprehensive characterization of three classes of Arabidopsis SW/SNF chromatin remodelling complexes. Nature Plants 8: 1423–1439.

Google Scholar: [Author Only](#) [Title Only](#) [Author and Title](#)

Guo P, Hoang N, Sanchez J, Zhang EH, Rajawasam K, Trinidad K, Sun H, Zhang H. 2022b. The assembly of mammalian SW/SNF chromatin remodeling complexes is regulated by lysine-methylation dependent proteolysis. Nature Communications 13: 6696.

Google Scholar: [Author Only](#) [Title Only](#) [Author and Title](#)

Han S-K, Sang Y, Rodrigues A, BIOL425 F2010, Wu M-F, Rodriguez PL, Wagner D. 2012. The SW2/SNF2 Chromatin Remodeling ATPase BRAHMA Represses Abscisic Acid Responses in the Absence of the Stress Stimulus in Arabidopsis. The Plant Cell 24: 4892–4906.

Google Scholar: [Author Only](#) [Title Only](#) [Author and Title](#)

Hauvermale AL, Tuttle KM, Takebayashi Y, Seo M, Steber CM. 2015. Loss of Arabidopsis thaliana Seed Dormancy is Associated with Increased Accumulation of the GID1 GA Hormone Receptors. Plant and Cell Physiology 56: 1773–1785.

Google Scholar: [Author Only](#) [Title Only](#) [Author and Title](#)

He H, Willems LAJ, Batushansky A, Fait A, Hanson J, Nijveen H, Hilhorst HWM, Bentsink L. 2016. Effects of Parental Temperature and Nitrate on Seed Performance are Reflected by Partly Overlapping Genetic and Metabolic Pathways. Plant and Cell Physiology 57: 473–487.

Google Scholar: [Author Only](#) [Title Only](#) [Author and Title](#)

Hernández-García J, Diego-Martin B, Kuo PH, Jami-Alahmadi Y, Vashisht AA, Wohlschlegel J, Jacobsen SE, Blázquez MA, Gallego-Bartolomé J. 2022. Comprehensive identification of SW/SNF complex subunits underpins deep eukaryotic ancestry and reveals new plant components. Communications Biology 5: 549.

Google Scholar: [Author Only](#) [Title Only](#) [Author and Title](#)

Holdsworth MJ, Bentsink L, Soppe WJJ. 2008. Molecular networks regulating Arabidopsis seed maturation, after-ripening, dormancy and germination. New Phytologist 179: 33–54.

Google Scholar: [Author Only](#) [Title Only](#) [Author and Title](#)

Hurtado L, Farrona S, Reyes JC. 2006. The putative SW/SNF complex subunit BRAHMA activates flower homeotic genes in Arabidopsis thaliana. Plant Molecular Biology 62: 291–304.

Google Scholar: [Author Only](#) [Title Only](#) [Author and Title](#)

Ibarra SE, Tognacca RS, Dave A, Graham IA, Sánchez RA, Botto JF. 2016. Molecular mechanisms underlying the entrance in secondary dormancy of *Arabidopsis* seeds: Mechanisms underlying secondary dormancy. *Plant, Cell & Environment* 39: 213–221.

Google Scholar: [Author Only](#) [Title Only](#) [Author and Title](#)

Iwasaki M, Penfield S, Lopez-Molina L. 2022. Parental and Environmental Control of Seed Dormancy in *Arabidopsis thaliana*. *Annual Review of Plant Biology* 73: 355–378.

Google Scholar: [Author Only](#) [Title Only](#) [Author and Title](#)

Jarończyk K, Sosnowska K, Zaborowski A, Pupel P, Bucholc M, Małecka E, Siwirykow N, Stachula P, Iwanicka-Nowicka R, Koblowska M, et al. 2021. Bromodomain-containing subunits BRD1, BRD2, and BRD13 are required for proper functioning of SWI/SNF complexes in *Arabidopsis*. *Plant Communications* 2: 100174.

Google Scholar: [Author Only](#) [Author and Title](#)

Jégu T, Veluchamy A, Ramirez-Prado JS, Rizzi-Paillet C, Perez M, Lhomme A, Latrasse D, Coleno E, Vicaire S, Legras S, et al. 2017. The *Arabidopsis* SWI/SNF protein BAF60 mediates seedling growth control by modulating DNA accessibility. *Genome Biology* 18: 114.

Google Scholar: [Author Only](#) [Title Only](#) [Author and Title](#)

Koramutla MK, Negi M, Ayele BT. 2021. Roles of Glutathione in Mediating Abscisic Acid Signaling and Its Regulation of Seed Dormancy and Drought Tolerance. *Genes* 12: 1620.

Google Scholar: [Author Only](#) [Title Only](#) [Author and Title](#)

Krzyszton M, Sacharowski SP, Sanchez F, Muter K, Dobisova T, Swiezewski S. 2022. Single seeds exhibit transcriptional heterogeneity during secondary dormancy induction. *Plant Physiology* 190: 211–225.

Google Scholar: [Author Only](#) [Title Only](#) [Author and Title](#)

Kumar S, Kaur A, Chattopadhyay B, Bachhawat AK. 2015. Defining the cytosolic pathway of glutathione degradation in *Arabidopsis thaliana*: role of the ChaC/GCG family of γ -glutamyl cyclotransferases as glutathione-degrading enzymes and AtLAP1 as the Cys-Gly peptidase. *Biochemical Journal* 468: 73–85.

Google Scholar: [Author Only](#) [Title Only](#) [Author and Title](#)

Lefebvre V, North H, Frey A, Sotta B, Seo M, Okamoto M, Nambara E, Marion-Poll A. 2006. Functional analysis of *Arabidopsis* NCED6 and NCED9 genes indicates that ABA synthesized in the endosperm is involved in the induction of seed dormancy. *The Plant Journal* 45: 309–319.

Google Scholar: [Author Only](#) [Title Only](#) [Author and Title](#)

Li T, Zhang Y, Wang D, Liu Y, Dirk LMA, Goodman J, Downie AB, Wang J, Wang G, Zhao T. 2017. Regulation of Seed Vigor by Manipulation of Raffinose Family Oligosaccharides in Maize and *Arabidopsis thaliana*. *Molecular Plant* 10: 1540–1555.

Google Scholar: [Author Only](#) [Title Only](#) [Author and Title](#)

Mashtalir N, D'Avino AR, Michel BC, Luo J, Pan J, Otto JE, Zullow HJ, McKenzie ZM, Kubiak RL, St. Pierre R, et al. 2018. Modular Organization and Assembly of SWI/SNF Family Chromatin Remodeling Complexes. *Cell* 175: 1272-1288.e20.

Google Scholar: [Author Only](#) [Title Only](#) [Author and Title](#)

Mhamdi A, Hager J, Chaouch S, Queval G, Han Y, Taconnat L, Saindrenan P, Gouia H, Issakidis-Bourguet E, Renou J-P, et al. 2010. *Arabidopsis* GLUTATHIONE REDUCTASE1 Plays a Crucial Role in Leaf Responses to Intracellular Hydrogen Peroxide and in Ensuring Appropriate Gene Expression through Both Salicylic Acid and Jasmonic Acid Signaling Pathways. *Plant Physiology* 153: 1144–1160.

Google Scholar: [Author Only](#) [Title Only](#) [Author and Title](#)

Montez M, Majchrowska M, Krzyszton M, Bokota G, Sacharowski S, Wrona M, Yatusevich R, Massana F, Plewczynski D, Swiezewski S. 2023. Promoter-pervasive transcription causes RNA polymerase II pausing to boost DOG1 expression in response to salt. *The EMBO journal* 42: e112443.

Google Scholar: [Author Only](#) [Title Only](#) [Author and Title](#)

Nguyen T-P, Cueff G, Hegedus DD, Rajjou L, Bentsink L. 2015. A role for seed storage proteins in *Arabidopsis* seed longevity. *Journal of Experimental Botany* 66: 6399–6413.

Google Scholar: [Author Only](#) [Title Only](#) [Author and Title](#)

Nguyen T-P, Keizer P, Van Eeuwijk F, Smekens S, Bentsink L. 2012. Natural Variation for Seed Longevity and Seed Dormancy Are Negatively Correlated in *Arabidopsis*. *Plant Physiology* 160: 2083–2092.

Google Scholar: [Author Only](#) [Title Only](#) [Author and Title](#)

Nguyen VPT, Stewart J, Lopez M, Ioannou I, Allais F. 2020. Glucosinolates: Natural Occurrence, Biosynthesis, Accessibility, Isolation, Structures, and Biological Activities. *Molecules* 25: 4537.

Google Scholar: [Author Only](#) [Title Only](#) [Author and Title](#)

Ojolo SP, Cao S, Priyadarshani SVGN, Li W, Yan M, Aslam M, Zhao H, Qin Y. 2018. Regulation of Plant Growth and Development: A Review From a Chromatin Remodeling Perspective. *Frontiers in Plant Science* 9: 1232.

Google Scholar: [Author Only](#) [Title Only](#) [Author and Title](#)

Omidbakhshfard MA, Winck FV, Arvidsson S, Riaño-Pachón DM, Mueller-Roeber B. 2014. A step-by-step protocol for formaldehyde-assisted isolation of regulatory elements from *Arabidopsis thaliana*. *Journal of Integrative Plant Biology* 56: 527–538.

Google Scholar: [Author Only](#) [Title Only](#) [Author and Title](#)

Ranganathan U, Groot SPC. 2023. Seed Longevity and Deterioration. In: Dadlani M, Yadava DK, eds. *Seed Science and Technology*. Singapore: Springer Nature Singapore, 91–108.

Google Scholar: [Author Only](#) [Title Only](#) [Author and Title](#)

Rosnoblet C, Aubry C, Leprince O, Vu BL, Rogniaux H, Buitink J. 2007. The regulatory gamma subunit SNF4b of the sucrose non-fermenting-related kinase complex is involved in longevity and stachyose accumulation during maturation of *Medicago truncatula* seeds. *The Plant Journal* 51: 47–59.

Google Scholar: [Author Only](#) [Title Only](#) [Author and Title](#)

Sacharowski SP, Gratkowska DM, Sarnowska EA, Kondrak P, Jancewicz I, Porri A, Bucior E, Rolicka AT, Franzen R, Kowalczyk J, et al. 2015. SWP73 Subunits of Arabidopsis SW/SNF Chromatin Remodeling Complexes Play Distinct Roles in Leaf and Flower Development. *The Plant Cell* 27: 1889–1906.

Google Scholar: [Author Only](#) [Title Only](#) [Author and Title](#)

Sajeev N, Koornneef M, Bentsink L. 2024. A commitment for life: Decades of unraveling the molecular mechanisms behind seed dormancy and germination. *The Plant Cell*: koad328.

Google Scholar: [Author Only](#) [Title Only](#) [Author and Title](#)

Salvi P, Varshney V, Majee M. 2022. Raffinose family oligosaccharides (RFOs): role in seed vigor and longevity. *Bioscience Reports* 42: BSR20220198.

Google Scholar: [Author Only](#) [Title Only](#) [Author and Title](#)

Sano N, Marion-Poll A. 2021. ABA Metabolism and Homeostasis in Seed Dormancy and Germination. *International Journal of Molecular Sciences* 22: 5069.

Google Scholar: [Author Only](#) [Title Only](#) [Author and Title](#)

Sano N, Rajjou L, North HM, Debeaujon I, Marion-Poll A, Seo M. 2016. Staying Alive: Molecular Aspects of Seed Longevity. *Plant and Cell Physiology* 57: 660–674.

Google Scholar: [Author Only](#) [Title Only](#) [Author and Title](#)

Schymanski EL, Jeon J, Gulde R, Fenner K, Ruff M, Singer HP, Hollender J. 2014. Identifying Small Molecules via High Resolution Mass Spectrometry: Communicating Confidence. *Environmental Science & Technology* 48: 2097–2098.

Google Scholar: [Author Only](#) [Title Only](#) [Author and Title](#)

Shang J, He X. 2022. Chromatin-remodeling complexes: Conserved and plant-specific subunits in *Arabidopsis*. *Journal of Integrative Plant Biology* 64: 499–515.

Google Scholar: [Author Only](#) [Title Only](#) [Author and Title](#)

Skubacz A, Daszkowska-Golec A. 2017. Seed Dormancy: The Complex Process Regulated by Abscisic Acid, Gibberellins, and Other Phytohormones that Makes Seed Germination Work. In: El-Esawi M, ed. *Phytohormones - Signaling Mechanisms and Crosstalk in Plant Development and Stress Responses*. InTech.

Google Scholar: [Author Only](#) [Title Only](#) [Author and Title](#)

Stachula P, Kapela K, Malecka E, Jaronczyk K, Patryn J, Siwirykow N, Bucholc M, Marczak M, Kotlinski M, Archacki R. 2023. BRM Complex in *Arabidopsis* Adopts ncBAF-like Composition and Requires BRD Subunits for Assembly and Stability. *International Journal of Molecular Sciences* 24: 3917.

Google Scholar: [Author Only](#) [Title Only](#) [Author and Title](#)

Stotz HU, Sawada Y, Shimada Y, Hirai MY, Sasaki E, Krischke M, Brown PD, Saito K, Kamiya Y. 2011. Role of camalexin, indole glucosinolates, and side chain modification of glucosinolate-derived isothiocyanates in defense of *Arabidopsis* against *Sclerotinia sclerotiorum*. *The Plant Journal* 67: 81–93.

Google Scholar: [Author Only](#) [Title Only](#) [Author and Title](#)

Tang X, Hou A, Babu M, Nguyen V, Hurtado L, Lu Q, Reyes JC, Wang A, Keller WA, Harada JJ, et al. 2008. The *Arabidopsis* BRAHMA chromatin-remodeling ATPase is involved in repression of seed maturation genes in leaves. *Plant Physiology* 147: 1143–1157.

Google Scholar: [Author Only](#) [Title Only](#) [Author and Title](#)

Tognacca RS, Botto JF. 2021. Post-transcriptional regulation of seed dormancy and germination: Current understanding and future directions. *Plant Communications* 2: 100169.

Google Scholar: [Author Only](#) [Title Only](#) [Author and Title](#)

Yatusevich R, Fedak H, Ciesielski A, Krzyczmonik K, Kulik A, Dobrowolska G, Swiezewski S. 2017. Antisense transcription represses *Arabidopsis* seed dormancy QTL DOG 1 to regulate drought tolerance. *EMBO reports* 18: 2186–2196.

Google Scholar: [Author Only](#) [Title Only](#) [Author and Title](#)

Yu X, Willmann MR, Vandivier LE, Trefely S, Kramer MC, Shapiro J, Guo R, Lyons E, Snyder NW, Gregory BD. 2021. Messenger RNA 5' NAD⁺ capping is a dynamic regulatory epitranscriptome mark that is required for proper response to abscisic acid in Arabidopsis. *Developmental Cell* 56: 125-140.e6.

Google Scholar: [Author Only](#) [Title Only](#) [Author and Title](#)

Yu Y, Liang Z, Song X, Fu W, Xu J, Lei Y, Yuan L, Ruan J, Chen C, Fu W, et al (2020) BRAHMA-interacting proteins BRIP1 and BRIP2 are core subunits of Arabidopsis SWI/SNF complexes. *Nat Plants* 6: 996–1007

Google Scholar: [Author Only](#) [Title Only](#) [Author and Title](#)

Yu Y, Fu W, Xu J, Lei Y, Song X, Liang Z, Zhu T, Liang Y, Hao Y, Yuan L, et al (2021) Bromodomain-containing proteins BRD1, BRD2, and BRD13 are core subunits of SWI/SNF complexes and vital for their genomic targeting in Arabidopsis. *Molecular Plant* 14: 888–904

Google Scholar: [Author Only](#) [Title Only](#) [Author and Title](#)

Zinsmeister J, Leprince O, Buitink J. 2020. Molecular and environmental factors regulating seed longevity. *Biochemical Journal* 477: 305–323.

Google Scholar: [Author Only](#) [Title Only](#) [Author and Title](#)

Zumsteg J, Bossard E, Gourguillon L, Villette C, Heintz D. 2023. Comparison of nocturnal and diurnal metabolomes of rose flowers and leaves. *Metabolomics* 20: 4.

Google Scholar: [Author Only](#) [Title Only](#) [Author and Title](#)

ACCEPTED MANUSCRIPT